To the Graduate Council:

I am submitting herewith a thesis written by Matthew P. Duran entitled “Production and Optimization of Continuous Roving-Like UTSI Pitch based Carbon Fiber Composites." I have examined the final electronic copy of this thesis for form and content and recommend that it be accepted in partial fulfillment of the requirements for the degree of Masters of Science, with a major in Mechanical Engineering.

Ahmad D. Vakil

Major Professor

We have read this thesis

and recommend its acceptance:

Zhogren Yue

Basil N. Antar

Accepted for the Council:

Carolyn R. Hodges

Vice Provost and Dean of the Graduate School

(Original signatures are on file with official student records.)

Production and Optimization of Continuous Roving-like UTSI Pitch-based Carbon Fiber Composites

A Thesis

Presented for the

Masters of Science

Degree

The University of Tennessee, Knoxville

Matthew P. Duran

August 2009

ABSTRACT

UTSI has developed a new low-cost jet-dry-spin method for the production of mesophase pitch-based carbon fibers. The objective of this preliminary study is to optimize the production of the UTSI carbon fiber composites and to better understand the surface texture between the fiber and matrix material. Several fabrication techniques were studied with varied preparation conditions to determine the effects on apparent density, electrical resistivity, tensile and flexural properties. Various polymeric resins and hardeners were used to demonstrate the versatility of the application of UTSI carbon fibers. During these investigations various analysis techniques including Scanning Electron Microscopy (SEM), x-ray diffraction, and optical microscope aided in the determination of the structural characteristics of the fiber and its composite.

It was found that vacuum bagging resin infusion is the optimal fabrication process due to its ability to minimize porosity and increase fiber volume/content. The use of extra slow hardener allowed excellent control over the wetting, degassing, and cure time. Increasing applied pressure during the fabrication of the composites increases the fiber content/volume leading to improvements in mechanical properties, apparent density and electrical conductivity. However, excessive pressure causes difficult diffusion of the resin and the crash of carbon fibers which decrease the above properties. A preliminary work also shows that low cost phenolic resin composites and converted C/C composites can be easily prepared using UTSI CF.

Fiber surface oxidative treatments with ozone and HNO_3 solution were performed for comparison and optimization. Single-fiber fragmentation tests including single-fiber tensile/diameter testing revealed improvements in interfacial shear strength between oxidized carbon fiber (CF) and epoxy resin. Ozone treatment proved to be optimal, increasing flexure strength two-fold with respect to composites fabricated using as received CF.

DEDICATION

This thesis is dedicated to my family and friends particularly friends both present and abroad from UTSI. It is to them I owe the honor of attaining two Masters. They have made my stay at the University of Tennessee Space Institute both pleasant and memorable. I would also like to thank Justin Carpenter for encouraging me to continue learning and giving me the drive to attain my childhood dreams of becoming a scientist.

I would like to express deep gratitude to my major advisor Dr. Ahmad Vakili. He has given me the chance to grow professionally and has provided a great example to follow. I would also like to express my sincere thanks to Dr. Zhongren Yue for his valuable questioning and suggestions which have given me better insight into my work. I would also like to express my gratitude to all members of my thesis committee: Dr. A. Vakili, Dr. Z. Yue, and Dr. B. Antar. A special thanks goes to the Federal Transit Administration (FTA), and the Department of Transportation (DoT) for their support and for contract No. TN-26-7029-00.

TABLE OF CONTENTS

LIST OF TABLES

LIST OF FIGURES

LIST OF ABBREVIATIONS

ASTM	American Standard Test Methods International
C/C	Carbon-Carbon
CF	Carbon Fiber
CFC	Carbon Fiber Composites
CL	Critical Length
CTE	Coefficient of Thermal Expansion
DoT	Department of Transportation
FTA	Federal Transit Administration
IFSS	Interfacial Shear Strength
PAN	Polyacrylonitrile
SEM	Scanning Electron Microscopy
UTSI	University of Tennessee Space Institute
VB	Vacuum Bagging
VBRI	Vacuum Bagging Resin Infusion

Chapter 1: Introduction

Carbon Fibers and Their Composites

Carbon fiber (CF) dates back to 1879. Inventor, Thomas Edison, used carbon fibers as filaments for early light bulbs. Although these fibers lacked the tensile strength of today's carbon fibers, their considerable tolerance to heat made these fibers ideal for conducting electricity. Edison's carbon fibers were made out of cellulose-based materials, such as cotton or bamboo, unlike the petroleum-based precursors used today. Carbonization took place by baking bamboo filaments at high temperatures in a controlled atmosphere. This is a method known as "pyrolysis," which is still used today. The resulting carbonized bamboo filaments were fire-resistant and capable of enduring the intense heat needed for incandescence.

It wasn't until the late 1950's that high tensile strength carbon fibers were discovered. Rayon became the first precursors used to create these modern fibers. Ultimately, it was replaced by more effective materials such as polyacrylonitrile (PAN) and pitch. The benefits of these high-strength fibers were clear. Their weight is a fraction of steel’s yet contained much greater tensile strength than steel. Another important benefit of carbon fiber was its high modulus, or resistance to stretching. This inelasticity plays an important role in reinforcing rigid structures such as the nose cones in hypersonic aircraft.

Carbon fibers are classified by tensile modulus. Low modulus fibers have modulus > 240 GPa while intermediate through ultrahigh are between 500 -100 GPa. To give a better understanding of the strengths of carbon fibers consider the modulus of steel. Steel has a modulus of 200 GPa. When compared to ultrahigh carbon fibers it is easy to see that steel is five times weaker.

Ultrahigh modulus fibers are made from petroleum pitch. The pitch is treated such that the fibers crystalline structure is graphitic. Graphite is a pure form of carbon, its structure an allotrope just the same as diamond.

About 90% of carbon fibers are made from polyacrylonitrile. The rest are produced from rayon or petroleum pitch. The process of producing carbon fibers is both chemical and mechanical in nature. A typical sequence of operations used to form carbon fibers is as follows [1]:

A. Spinning. Precursors such as PAN or Pitch are spun into fibers by mixing with certain chemicals and forced through tiny jets into a chemical bath or quench chamber. Here the mix coagulates and solidifies in to the resulting fibers. Other methods heat the mixture while pumping it through tiny jets into a chamber where the solvents evaporate. The remaining material is the fiber. The internal atomic structure of the fiber is determined by the spinning process. It is this very reason that much research has been done in this step alone. The fibers are then washed and stretched to a desired diameter. This stretching aids in the alignment of the molecules within the fiber, effectively creating tightly bonded carbon crystals when carbonized.

B. Stabilizing. Inherently the resulting fibers are thermally unstable. it was because initial fibers decomposed during heat treatments that initial research was halted. The fibers must be chemically treated to thermally stabilize the atomic bonding. The solution is to heat them at about 200-350°C for several minutes. This allows oxygen to diffuse into the atomic structure increasing the strength of the bonds and its thermal stability.

C. Carbonizing. The next step is to heat the fibers between 1,000 to 3,000°C for several minutes. In order to prevent decomposition an inert gas is used. This removes any non-carbon atoms from the atomic structure such as water vapor, carbon monoxide, carbon dioxide, and hydrogen. The resulting fiber will have tightly bonded crystalline structures with better alignment perpendicular to the fiber axis.

D. Treating the surface. The drawback with having tightly bonded crystal structures is that they are inherently inert themselves. Of specific nuisance is the inert surface of carbonized fibers. This is bad when trying to combine fibers and matrix materials. The surface must be slightly oxidized to provide better chemical bonding properties. These processes also etch and roughen the surface giving more surface

area for bonding. Ideal gases for oxidizing are air, carbon dioxide, and ozone. Ideal liquids include sodium hypochlorite or nitric acid. Electrolysis can also be used by coating the fibers when treating them as a positive terminal in a bath of electrically conductive materials. Warning must be given to producing surface defects which could be sources of failure.

E. Sizing. Now that the fibers have been surface treated, they must undergo a process called sizing where they are coated to protect them from damage during winding or weaving. Typical coating materials are epoxy, polyester, nylon, and urethane.

In recent decades, carbon fibers have found wide application in commercial and civilian aircraft, recreational, industrial, and transportation markets. Carbon fibers are used in composites with a lightweight matrix. Carbon fiber composites are ideally suited to applications where strength, stiffness, lower weight, and outstanding fatigue characteristics are critical requirements. They also can be used in the occasion where high temperature durability, chemical inertness and high damping are important.

Problems and Objective

Despite the popularity of PAN fiber for possessing great mechanical properties, it still requires high cost due to the value of the precursors and chemicals needed for the spin process. This detracts from its use in commercial applications. It also leads to the use of such fibers only when cost is not a major factor. Currently, commercially available carbon fiber composites make up 50% of the Boeing 787. Unfortunately the high cost of this same material prevents its use in car body material. The core of this problem is the scarcity and high cost of PAN precursor material.

The only solution is to focus research on new methods for producing low-cost carbon fibers and composites. New abundant and cheap natural materials and petroleum pitch are being investigated for use in making low-cost carbon fibers. One plus is that the pitch has a very high carbon yield. Despite more than 25 years of

research on pitch-based carbon fibers, only cheap low performance fibers have been developed. All high performance fibers produced are high in cost.

The University of Tennessee Space Institute (UTSI) has implemented research into low-cost carbon fiber technology with funding from the (FTA), and DOT. The program name is “Low Cost Carbon Fiber Technology for Carbon Fiber Composite Applications”. Our goal is to produce the best possible CFCs using UTSI’s low-cost carbon fibers for use in the production of material technologies needed for existing and future endeavors.

Our low cost carbon fibers may provide superior cost effectiveness in the manufacturing of future carbon-based products to be used in everyday life. The commercially unfeasible technologies of today will be the technological breakthroughs of tomorrow. One example is the huge savings in energy consumption that would be made possible using high strength low weight body structures within the Automobile industry.

Scope of Present Work

It was the donation of Conoco Phillips’ carbon fiber spinning technologies in December of 2004 that made possible UTSI’s low cost carbon fiber research. The carbon fiber research lab directed by Dr. Ahmad Vakili uses mesophase pitch to produce fibers of comparable properties to that of existing commercially available carbon fiber. The difference being that UTSI carbon fibers are spun into a continuous weaving (see

Figure 1.1). Commercial carbon fibers are typically in tow or fabric form. These forms give additional strength by more evenly distributing load from fiber to fiber.

Once the spin group produces UTSI woven carbon fiber, we are faced with a question: How can we optimize the production process of carbon fibers composite material? The goal of this research is to lay the foundation for future material research by determining the best fabrication processes for CFC with specified mechanical requirements. Once this is accomplished we must determine how to control fabrication

parameters in order to take things a step further. We desire composite material with optimal overall mechanical properties.

The following six steps were taken to accomplish the above goals for UTSI carbon fiber research.

(1) Compared two fabrication methods, vacuum bagging and vacuum bagging with resin infusion, in order to obtain appropriate process for UTSI carbon fiber composites.

(2) Investigated the effect of the fabrication parameters, such as pressure, on mechanical and other physical (apparent density, e-conductivity) properties of the carbon fiber composites in order to optimize the fabrication process.

(3) Fabricated two polymer matrix, epoxy and phenolic resin composites, and preliminarily tested the conversion of phenolic resin/CF composites to carbon /CF composites in order to explore the possibility for the formation of various carbon fiber composites.

(4) Characterized the microstructure of the mesophase pitch-based carbon fiber by using SEM and X-ray diffraction and performed fiber surface treatments with ozone and nitric acid.

(5) Measured and compared the fiber critical length (CL) and the interfacial shear strength (IFSS) of the carbon fibers prior to and after surface treatments within epoxy resin by means of single fiber fragmental tests.

(6) Evaluated the composites made from the carbon fibers prior to and after surface treatments in order to see the improvement in mechanical properties.

Figure 1.1 Form of UTSI Carbon Fibers

Literature Review

M. Khan and A. Barron describe several applications and the obstacles facing them in their article “Carbon Fibers: Opportunities and Challenges” [2]. The search for cheap, strong, and easy to produce matrix materials are needed to satisfy the demands of future Aerospace and transportation projects around the world. It was during the 1970’s that work to find alternative raw materials led to the introduction of carbon fibers made from petroleum pitch-derived from oil processing. According to Zoltek [1], these fibers contained about 85% carbon and had excellent flexural strength. Today, carbon fibers are an important part of many products and new applications are being developed every year. The United States, Japan, and Western Europe are the leading producers of carbon fibers. UTSI has developed a dry-jet spinning method which produces a continuous webbing. Typically this spin method only produced short fibers. The attractiveness of dry jet spinning is that it requires less materials for the coagulation and solidification since it uses hot air. Thus UTSI has produces a new carbon fiber spin method whose production methods and product fit many of the needs for future applications, particularly those of the Tennessee Department of Transportation.

Much of the mechanical testing procedures follow chapter three of the Composite Materials Handbook [3]. The title of this chapter is “Evaluation of Reinforcement Fibers”. In this chapter various techniques and test methods are described that are typical in the characterization of chemical, physical, and mechanical properties of reinforcement fibers for application in organic matrix composite materials. Various types of fiber reinforcements are covered such as unidirectional yarns, strands, or tows, and bidirectional fabrics.

Secondary testing investigates the interfacial shear strength between the fiber and matrix. H. Hatta, K. Goto, and T. Aoki [4] describe several testing methods which include, tensile, shear and compressive loading that are commonly used. The most simpler of these methods being tensile loading as carbon fibers lack the ability to

withstand compressive loading and such testing is generally very difficult to undertake given the typical size of the fiber. Tensile testing, on the other hand, can be readily done with small samples and requires light loads. Testing procedures follow those of Rise National Laboratory's AFM department for material research [5]. The goal is to determine the optimal surface treatment method for producing good CFC. The role of interfacial shear strength is discussed in detail by H. Hatta and K. Goto, and T. Aoki [4].

Variety of classifications for matrix materials called the continuous phase are used for the creation of fiber-reinforced composites [6]. Three of these categories are polymeric matrix, mineral matrix and metallic matrix. Some examples of metallic matrix materials are aluminum alloys, titanium alloys, and oriented eutectics. Mineral matrix materials include silicon carbide and carbon. They can be used at high temperatures, which is ideal for rocket propulsion and re-entry applications. Polymeric materials have two subcategories, thermoplastic and thermoset.

Thermoplastic resins are high molecular weight polymers whose chains are bonded with weak Van der Walls forces. Typically this means hydrogen bonding, dipole-dipole interactions, and stacking of aromatic rings. These thermoplastics are labeled such due to their ability to be remelted and remolded after curing. Some examples of these polymers are polyphenylene sulfone, polyamide, polyetheretherketone, and nylon.

Thermoset resins are polymer materials that irreversibly cure. This can be accomplished several ways, through heat, chemical reaction or irradiation. This process transforms the resin into a plastic or rubber by cross-linking the polyester, phenolic, melamines, silicones, polyurethanes, or epoxy chains. The chemically active sites bond into a rigid 3-D structure. Once this is accomplished the resin becomes one large solid molecule with a melting point higher than the surrounding ambient temperature.

D. Chung describes the chemical properties of resins in her book "Carbon Fiber Composites" [7]. The following paragraphs are an outline of the molecules and reactions involved when dealing with epoxy resins. Only the characteristics that are desirable for CFC research will be discussed.

Epoxy has low molecular weight when uncured and in such a state possesses an high molecular mobility. It is this mobility that enables resin to quickly wet the surface of carbon fiber. This is due to its chemical structure. Epoxy resins have two or more epoxide groups per molecule (See **Figure 1.2**). The chemical structure for most epoxies is shown in **Figure 1.3** where Be identifies the benzene rings.

Figure 1.4 shows the cross linking process. The epoxy and hydroxyl groups (-OH) are the reaction sites for cross-linking. These include amines, anhydrides, and aldehyde condensation materials. During curing the epoxide ring is split and a donor hydrogen from a member of the hydroxyl group bonds with the oxygen atom of the epoxide. In addition, shrinkage is low because the fact that there are no by-products during curing.

Phenolic resins can be categorized as two kinds:

1. A resole resin which is formed when reacting molar excesses of HCHO with alkaline catalyst. Further condensation forms ringed systems who's formations can be controlled to achieve the desired molecular weight distribution. This reactivity is dependant on the amount of methylol phenol groups (-CH_2OH-). In sum the more reactive the resin to acid catalysis, the shorter the cure time. The reaction can be sped up with higher temperatures between 120°C to 180°C decreasing the viscosity as well. Alternatively a cure can be achieved using a strong acid catalyst at ambient temperature.

A novalac resin is formed using a molar excess of phenol and acid catalyst. The simplest form of these is Bisphenol. These resins require a hardening agent to condense, agents such as hexamine will react to form HCHO. Once a suitable catalyst is used to stop the alcohol-epoxy reaction, the novalac resin can react with any epoxy groups through the existing phenolic -OH. This creates epoxy-novalacs which posses high molecular and epoxies to improve high temperature strength. Lower molecular weight novalac resins are very viscous at room temperature and can be blended with a diglycidyl ether of bisphenol A. They are cured by condensation reactions evolving H_2O.

Extra care must be taken to prevent water from remaining in the matrix during curing. this can be done with high pressure to avoid blistering and voids.

It is generally agreed that carbon fibers are composed of two-dimensional turbostratic graphitic crystallites. These Crystallites are generally orientated parallel to the fiber axis. The basic structural unit is a planar sheet composed of a hexagonal network of carbon atoms. A number of these layered aromatic planes, when aligned together, create what is called a crystallite or platelet. See **Figure 1.5** for visual reference. For PAN fibers the external surface or sheath has more ordered structure than the internal structure or core. Here the preferred orientation of the graphite sheets in the sheath is parallel to the fiber surface.

The surface morphology of carbon fibers is composed of many wrinkles or dips running almost along the fiber axis. It is because the crystal basal surfaces are completely bonded that the carbon atoms are practically chemically inert. Thus the more chemically active sites are located at incompletely bonded edges and faults in the structure. Thus the more completely graphitic and aligned the fiber's surface becomes the less potential there is for chemical bonding.

It is a known fact that most reinforcement fibers are surface treated to improve handability and/or promote fiber-resin bonding. Surface treatments affect wettability of the fiber during impregnation as well as the dry strength and hydrolytic stability of the fiber matrix bond during use. It is because of this direct relationship that the effectiveness of any treatments to modify surface chemistry is measured and generally measured on the composite itself. The sizing and its compositional consistency are significant in quality control of the fiber and measurement of these parameters is part of the fiber evaluation.

Although this thesis provides a great outline of testing procedures, it does not go into details to explain the physics or chemistry of how these various methods evaluate or improve fiber-epoxy bonding. Much of the modes by which bonding and failures

under loading occur are discussed in the text book “Fundamentals of Material Science and Engineering” [8]. In the fiber science class of Dr. Yue, detailed outlines of how good fiber reinforced composites are made and how to improve them are covered. Much of this thesis will be a confirmation of the theories presented in this class.

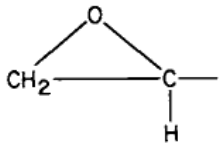

Figure 1.2 Typical Epoxide Molecule.

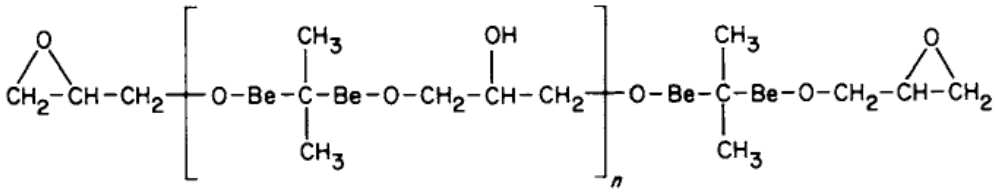

Figure 1.3 Typical Chemical Structure of Epoxies.

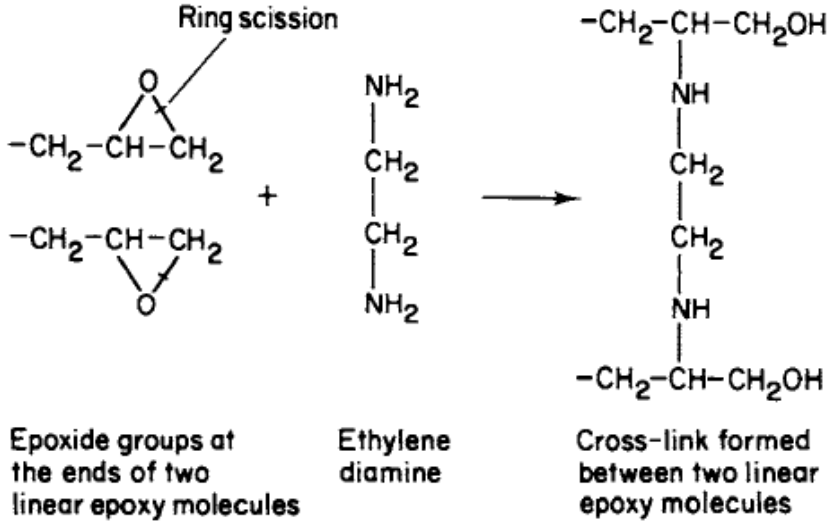

Figure 1.4 Cross Linking Process.

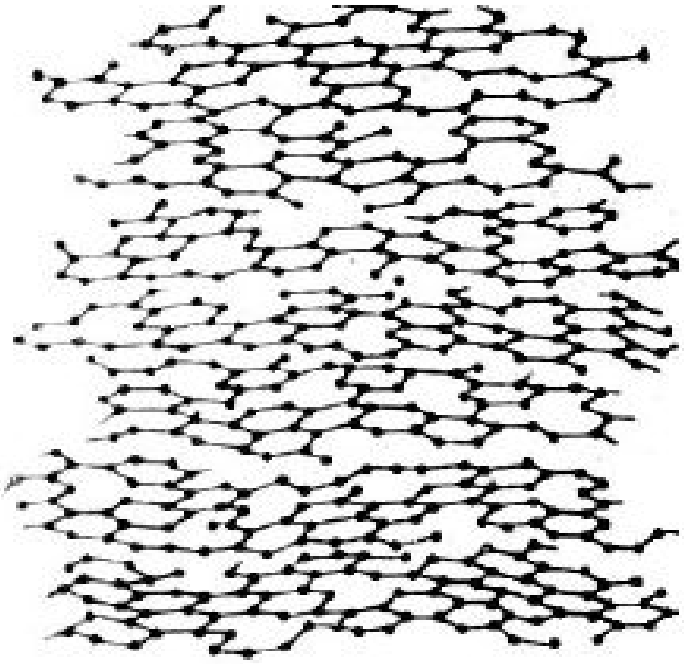

Figure 1.5 Turbostratic Graphite Structure.

Chapter 2: Materials and Methods

Materials

A: Carbon Fibers

Two forms of carbon fibers were employed in this study: 1) UTSI mesophase pitch-based carbon fibers produce in the UTSI spin lab. Their typical properties are listed in **Table 2.1**; 2) Commercial PAN-based fabric from Albany Engineered Composites. The fiber is a Techniweave Carbon Closed Edge Belt fabric; Serial Number: 1P3376-01-01-04; PO#: 4501386213; Style: 1148; and Product: 12" 10.5x10.5 4HS 12K.

Table 2.1 Typical Properties of the UTSI Carbon Fibers.

Carbonization Temperature (°C)	Fiber diameter (µm)	Tensile Strength (Mpa)	Tensile Modulus (Gpa)
1090	11.04	1070	108
1050	18.86	509	109

B: Matrix Materials

A variety of matrix materials such as epoxy, vinyl ester or polyester can be used for high-performance carbon fiber composites. An overview of previously conducted research, [7] indicated that epoxy resins would be ideal because of the following characteristics:

- Epoxy resins are known for incredible toughness and bonding strength,
- Quality epoxy resins can support reinforcements up to 2000 psi compared to 500 psi for vinyl ester resins and even less for polyester resins.
- Epoxy resins offer greater capability in flexing and straining with fibers without micro-fracturing.

- Cured epoxy tends to be very resistant to moisture absorption.
- Epoxy resins are compatible with all sorts of fibers, prevent delamination and offer excellent results in reparability whereas vinyl esters are great for glass fiber but do not work well with Kevlar and carbon fibers.
- Epoxy resins can bond dissimilar or cured materials making repairs that could be stronger and reliable.

For UTSI carbon fiber composites, epoxy resin 105 and extra slow hardener 209 produced by West System were used as matrix material. Initially we used slow hardener 206. The reason for using extra slow hardener was to aid in the elimination of gaseous bubbles by allowing more time for trapped air to escape via vacuum before the matrix hardened.

Phenolic resin was also used as a primary matrix material. Phenolic resins are used as initial bonding material for production of carbon/carbon composites. UTSI utilizes a phenolic resin produced by Georgia-Pacific Inc. It is readied in an alcohol solution, GPRI® BKS-2600, which contains some volatile solvents as ethanol, phenol, methanol, water, and formaldehyde. One must take care in removing these solvents when curing. If not, these solvents will gas up and become trapped to form voids.

C. Chemicals

(1) Nitric acid: HNO_3 certified ACS plus from Fisher Scientific of 69% assay was employed for carbon fiber surface treatment.

(2) Deionized (D. I.) water: DI water generated in the Chem Lab at the UTSI was used to wash the carbon fibers after HNO_3 oxidation.

Fabrication of Carbon Fiber Composites

The fabrication of carbon fiber composites was carried out at the UTSI Chem Lab. The following materials and instruments were used in the fabrication processes:

- A hot press, Model C, made by CARVER, inc.

- Vacuum bag kit includes vacuum caps, tubing, gauge, junction “T”bars, release fabric and breath fabric, bag film, and sealant. All was ordered from Jamestown Distributors.
- Two aluminum squares 5”x6” in dimension were cut and shaped by the UTSI machine shop and used as the molding plates to ensure the surface of the composite was smooth and shaped properly.
- Computype TS938 triacetate film was also used as the release film. It is smooth textured and allows the molding plates to be easily removed from the composite.

A: Vacuum Bagging

This first fabrication technique was a simple, standard vacuum bagging procedure which involved stretching 10-15 grams of carbon fiber onto a rolling pin and applying the epoxy resin through rolling. The epoxy impregnated carbon fiber is then placed between two metal molds. This "sandwich" was then placed inside a vacuum bag and sealed. The composite was then cured at room temperature under a vacuum of 27" Hg for 4 hours. This step is shown in **Figure 2.1**(below).

The second step was done using the hot press equipment as shown in **Figure 2.1**(bottom). Another steel plate (mold) was placed on the top of carbon fiber/epoxy. The carbon fiber/epoxy was further cured under pressure for 2 - 3 hours to make a carbon fiber/epoxy plate with smooth surfaces and a uniform thickness. When the material was near curing it was removed from the mold plates and placed in an oven overnight for final curing.

B: Vacuum Bagging Resin Infusion

Vacuum bagging resin infusion technique for making carbon fiber composites is shown in **Figure 2.2**. To avoid trapping air between layers of the wetted fiber resin infusion under vacuum was used to impregnate the fibers with epoxy resin; remove the air bubbles; and reduce excessive matrix resin. To improve fiber volume additional pressure was applied to the mold, compressing the fibers together.

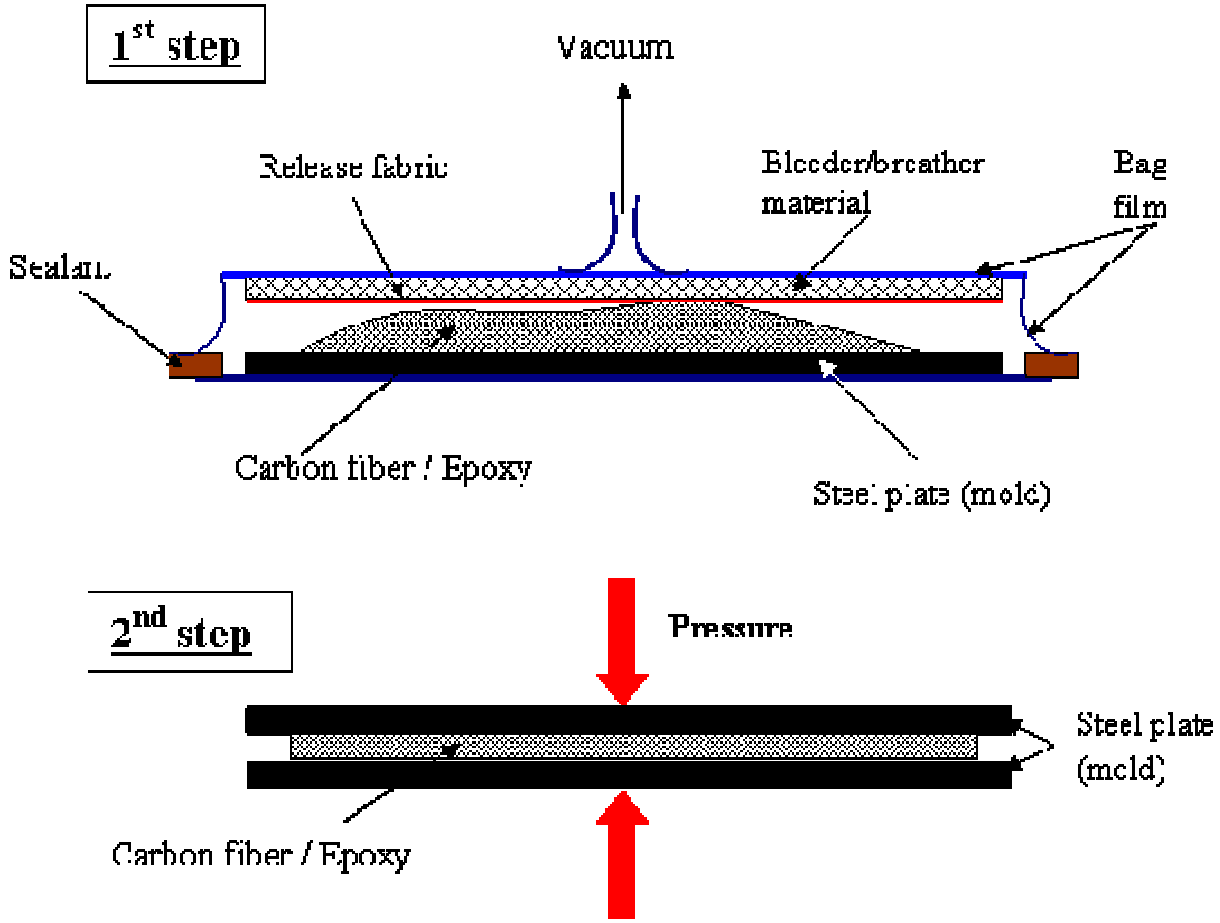

Figure 2.1 Vacuum Bagging Technique for Making Carbon Fiber/Epoxy Composites

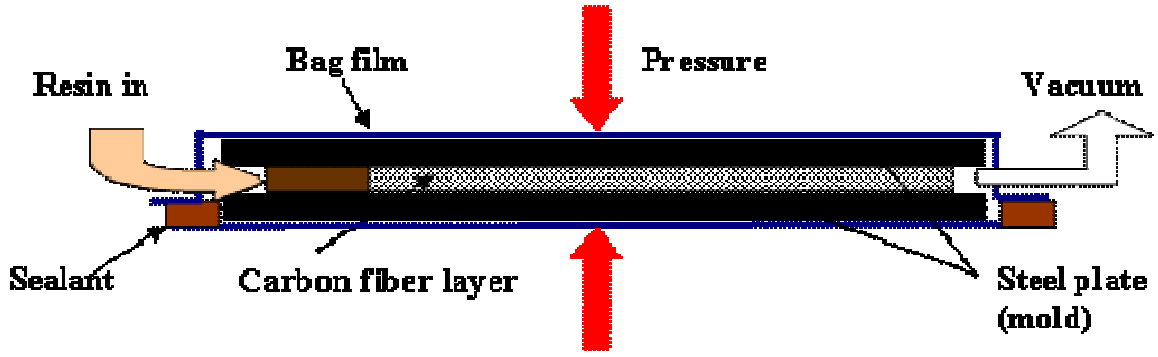

Figure 2.2 Vacuum Bagging Resin Infusion Technique for Making CFCs

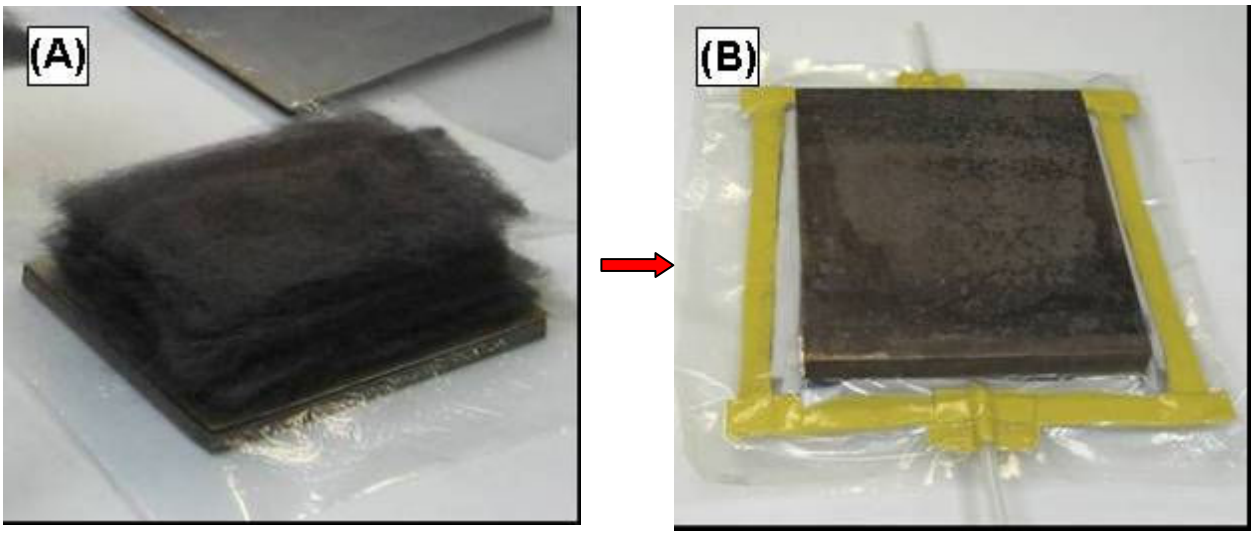

Figure 2.3 Carbon Fiber Packed in the Vacuum Bag

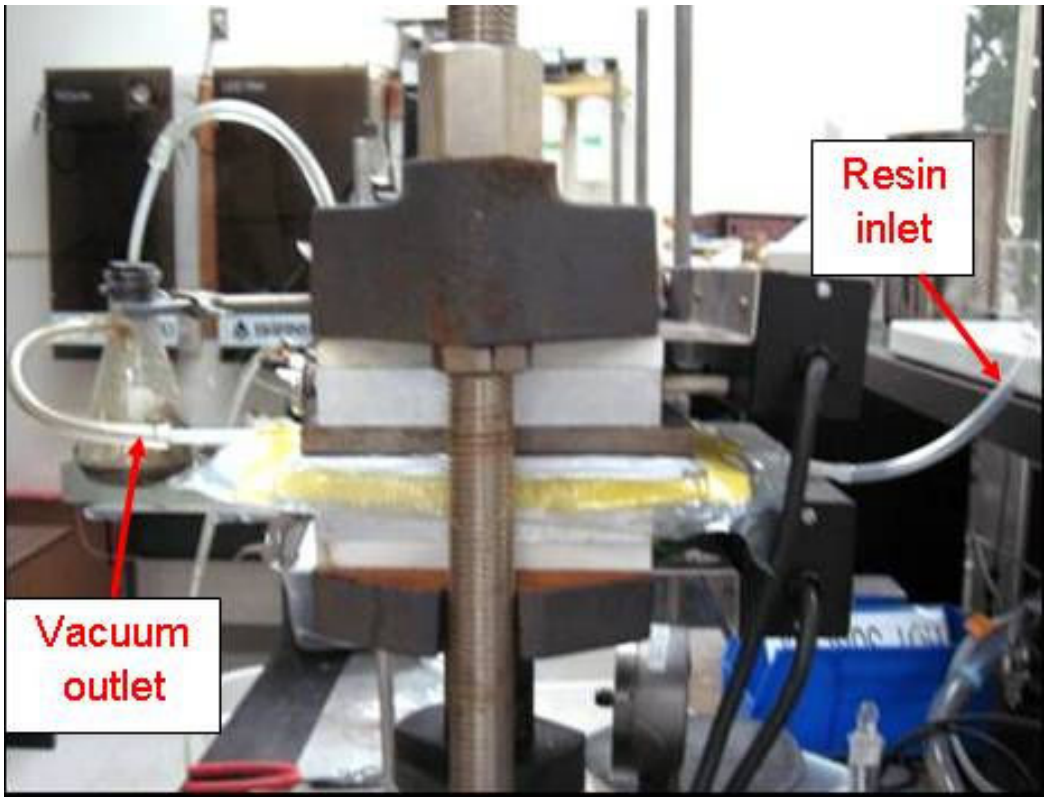

Figure 2.4 Setup for Vacuum Bagging Resin Infusion with Hot Press

The detail procedures for the vacuum bagging resin infusion technique are described as follows: The carbon fiber was stacked up on the plate (see **Figure 2.3** A). Both of them were then packed with bagging film and sealed four sides with sealants. Two plastic tubes were installed in the two sides of the plates. One was used as resin infusion inlet and another as vacuum outlet (see **Figure 2.3** B). The above system was then placed in a hot press as shown in **Figure 2.4**.

The fiber was wetted as the epoxy diffused into the mold under a vacuum of 29”Hg. This insured that the maximum amount of air would be removed between the carbon fibers. In order to increase the time for gasses to be removed, an extra slow hardener 209 was applied to cure the resin. During the resin infusion process, the fiber/epoxy mix was subjected to a pressure of 1 to 3 tons or higher based on the carbon fibers used. This ensured a higher fiber volume and a more uniform thickness. Sometime, the mold was heated between 40-50°C to decrease the viscosity of the resin and lessen the time of the diffusion process. After the resin infusion, stop the vacuum and let the epoxy resin cure under the pressure overnight.

In the case of fabrication of phenolic resin composites, two different fabrication processes were used in preparing phenolic resin composites. One is that after phenolic resin solution was diffused through the entire carbon fiber layer, without further removal of solvents (Degas process), a thermal reactive cross-linking was immediately conducted by increasing the hot-press pressure and temperatures. Another process that can be done after resin infusion, the residue solvents were removed by vacuum pump at elevated temperatures to 100^{o}C. After a completed degas process, the thermal cross-link process was carried out by increasing the hot-press pressure and temperatures.

C. Carbon/Carbon Composite

The carbon-carbon fiber composite was prepared by simply carbonizing the above phenolic resin composites at 1000^{o}C in N_2.

Precursor: phenolic resin composites fabricated with degas process

Heating rate: ~ 10^{o}C /min.

Carbonization time at 1000^{o}C : 30 min

Fiber Surface Treatments

A: HNO_3 Oxidation

15 grams of UTSI pitch CF was laid in a 250 ML Pyrex glass in an overlapping manner but unidirectional. 100 grams of nitric acid, heated to around 100°C functionalized the fibers. Treat the fibers for 120 minutes. Once the proper time has passed cool the fibers back to ambient temperature. Before the fibers can dry fill the glass with DI water, drain and refill. Repeat this process until the pH level of the water immersed fibers reaches 6 or the same level as the DI water. Set in an oven at around 150°C to dry.

B: Ozone Oxidation

Ozone treatment, a form of gaseous oxidation, was another typical treatment used by UTSI to increase the level of adhesion between the fiber and its matrix material.

An Air – Zone XT-6000 ozone air purifier was used in this study. This piece of equipment can output between 500 mg/hr to 6000 mg/hr. It also possesses a built in timer for controlled treatment. To raise the temperature of the gas and promote chemical reaction a furnace was used to house the matted fiber material. Temperature probes were placed such that the temperature could be accurately monitored and controlled. A setup for ozone oxidation is shown in

Figure 2.5.

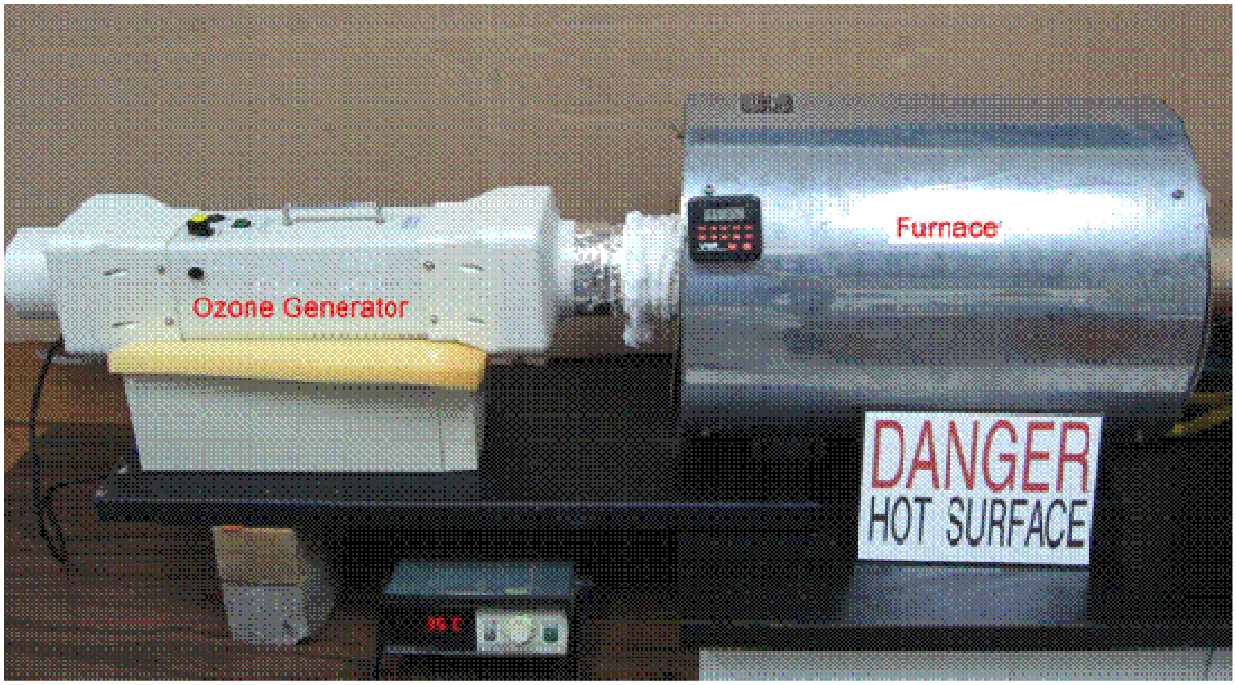

Figure 2.5 Reaction System for Ozone Oxidation**.**

Measurements and Characterization

A: Tensile Testing

Several batches of UTSI carbon fiber were used to produce a 5 x 6” composite plate. Form these plates six rectangular strips were cut with dimensions specified in test method ASTM D3039/D3039M [9]. The specimen is placed overnight into an oven at 150°C. The ends of theses strips were mounted with metal grips to easily be grasped by the MTS testing machine and monotonically loaded. The specimen preparation and tensile test setup were shown in **Figure 2.6**. Once the sample breaks the maximum load recorded before the brake is used to determine the composite strength. A strain gauge determines the strain experienced by the sample throughout the testing. The tensile samples were tested in an MTS machine with a 550 kN load cell and a head speed of 0.1 inch per minute. A precision extensometer as shown in **Figure 2.6** (right) was used to measure strain. The ASTM D3039/D3039M [9], standard was used as a guide to the testing and calculations reported (see **Appendix A**).

B: Flexural Testing

The flexural properties of carbon fiber composites was measured according to the standard test method by four-point bending, ASTM D6272 [10]. This test is applicable to CFC research since it is rigid and fails at the outer fibers. It employs a four-point load system to a simply supported beam.

The system uses four load noses with cylindrical surfaces of radius ≈ 5.0 mm. Two bottom noses provide the support for our specimen. The distance between them is determined from the support span-to-depth ratio which for us will be 32:1. This distance shall be called the support span. The two top noses are designated the load noses. The distance between theses noses are approximately one-third the support span. The loading diagram of 4-point bending testing is shown in **Figure 2.7**. To measure the deflection of the beam at the common center of the loading span, a precision extensometer was installed as shown in **Figure 2.7**. ASTM D6272 [10], standard was used as a guide for the testing and calculations reported (see **Appendix B**).

Figure 2.6 Specimen Preparation and Tensile Test Setup

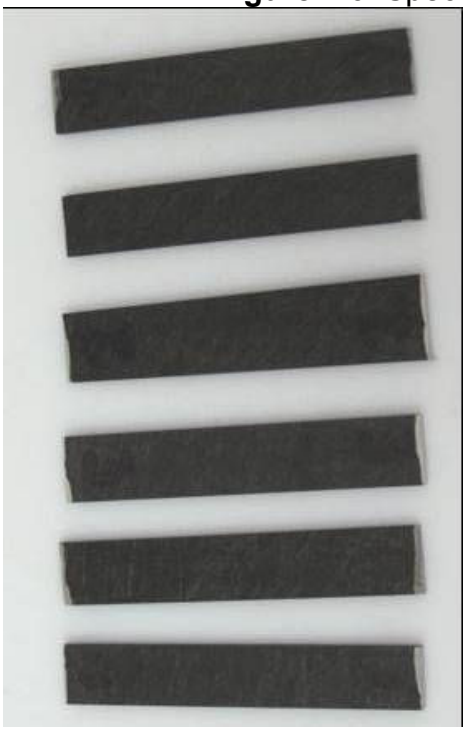

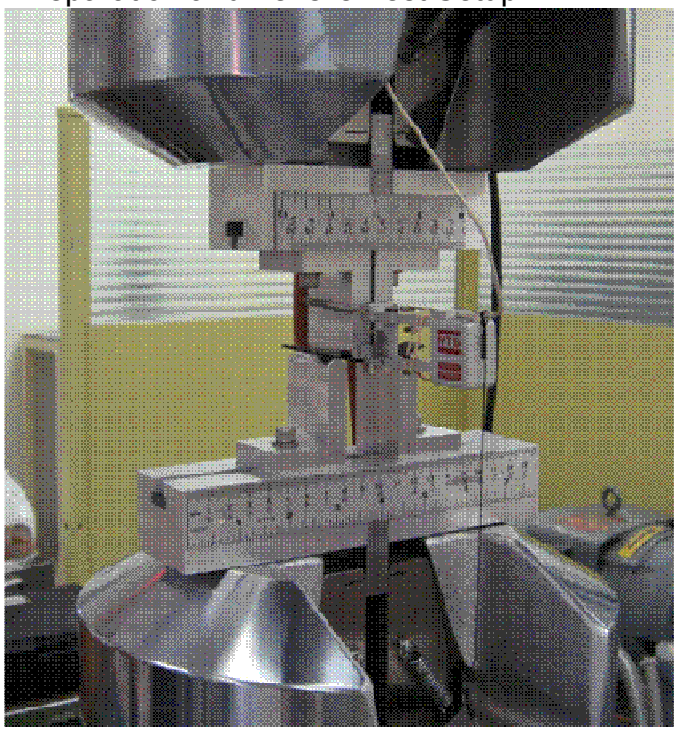

Figure 2.7 Specimen Preparation and Loading Diagram of 4-point Bending Testing.

Six bars of CFC were prepared for the flexural tests. The length of the bars was determined using the span-to-depth ratio which also include at each end at least 10% overhang. The widths of the bars do not exceed one-fourth of the length. Once they are cut and sanded they were placed overnight into an oven at 150°C. The following day they are placed in a desecator for cooling. Once they are at room temperature their weight and dimensions are measured and their apparent density (ρ) and electrical conductivity are then calculated first. These will be described later on the Part E. After that, the specimen prepared as shown in **Figure 2.7** (left) were tested for their flexural properties.

An MTS machine with a 550 kN load cell and a head speed of 0.1 inch per minute were used to measure the flexural strength, The flexural strength is evaluated by measuring the outer fiber stress and strain at the common center of the spans. An extensometer is attached to the MTS machine as seen **Figure 2.7** (right). For each specimen the support span as well as the width and depth at the common center are measured before placing the specimen into the MTS machine.

The load, deflection, and displacement from equilibrium were recorded periodically over time until the sample brakes. For each record we calculate the maximum fiber stress and strain using the formulas as follows:

$$S = \frac{p \times L}{b \times d^2} \tag{1}$$

$$r = 4.7 \times \frac{D \times d}{L^2} \tag{2}$$

Where ***S*** is the maximum fiber stress experienced by the outer fibers throughout the load span when a beam is loaded in flexure at two central points and supported at two outer points. The maximum fiber stress is measured in mega-Pascals. Let ***r*** define the maximum strain in the outer fibers at midspan to be measured in millimeter per millimeter. ***P*** is the load at a given point on the load-deflection curve measured in

Newtons. ***D*** is the maximum deflection of the center of the beam measured in millimeters. ***L*** is the support span measured in millimeters. Let ***b*** denote the width of the beam measured in millimeters. Finally ***d*** is the depth of the beam, also measured in millimeters.

Once these two equations are evaluated for every time point, a stress-strain curve for each specimen is able to be plotted, the flexural modulus and strength of the carbon fiber composite are then obtained.

C: Single-fiber Diameter and Tensile Testing

A vital part of determining the interfacial shear strength between the fiber and its matrix material is obtaining the average fiber tensile strength and fiber diameter. The tensile strength and diameter are continuously evaluated by single-filament test. The fiber analyzer instrument, FDAS765, by Diastron Limited, was employed in this study.

Diastron Limited FDAS765 fiber analyzer consisting of a high resolution tensile tester LEX810 with a force resolution of 0.005 gram and a Mitutoyo LSM-902 Laser Scan Micrometer with a positional repeatability of 0.1 microns. The FDAS765, automatically performs diameter measurements at several longitudinal points, records the elongation and calculates various parameters related to tensile fracture.

For each batch tested, six single carbon fiber samples were isolated from storage. Each six was cut roughly in half; half for single-fiber fragmentation testing (see next section) and half for tensile/diameter testing. For each tensile/diameter test fibers were cut into as many samples as can fit in two feet. At least three samples will do, but more samples yield better statistics. Individual fiber filaments are carefully mounted on special sample support mounts before their diameters are measured by a laser micrometer. Set the program to scan 10 slices per fiber piece and then begin the testing. Note: fiber length used for these test is 10 mm.

D: Fiber Fragment Testing

The purpose of this test is to evaluate the fiber critical length and the interfacial shear strength of the fibers to the matrix material. The procedure follows the test

methods of RisØ National Laboratory's "Testing procedure for the single fiber fragmentation test" [5].

Six dog bone molds were produced for fragmentation testing which is shown in **Figure 2.8** (left). The silicon rubber in conjunction with silica mold release spray allows for easy retrieval of cured samples.

The following is outlined from the single fiber fragmentation testing procedures. First isolate six long strands of fiber. As indicated in the above section, selected single fiber was cut roughly in half, half for tensile/diameter testing (see last section); half for single fiber fragmentation testing. Place the fiber straight and centered in the dog bone as shown in **Figure 2.8** (right). Apply tension to the fiber; this is important for good fracture testing.

Apply epoxy with a mix ratio of 1 part hardener and 5 parts resin. Once the epoxy is cured remove the samples from the mold. They will be roughly dog bone shaped and many deformations will be present on the surface. To make the samples uniform and transparent, sand the samples to the desired shape and polish to the desired transparency. The dog bones were approximately 1.88 x 0.5" in dimension with a neck 0.125" wide as shown in **Figure 2.9** (left).

Drill holes at each end of the polished samples and make sure they are placed evenly on each side to ensure equal amounts of stress threw out the testing. Once the holes are in place the sample is mounted to a mini tensile tester. **Figure 2.9** (right) shows the specimen mounted on the tensile tester apparatus.

Two marks are made to help calculate the critical length. One on each end of the dog bone neck. Once marked, the sample is placed in a Nikon Metaphot Optical Microscope with a cross-polarized light (see **Figure 2.10**) and the sample is incrementally stretched and the elongation and fractures are recorded. Pictures and movies can be taken using a digital camera and saved in a computer with Matrox Inspector 4.0 software.

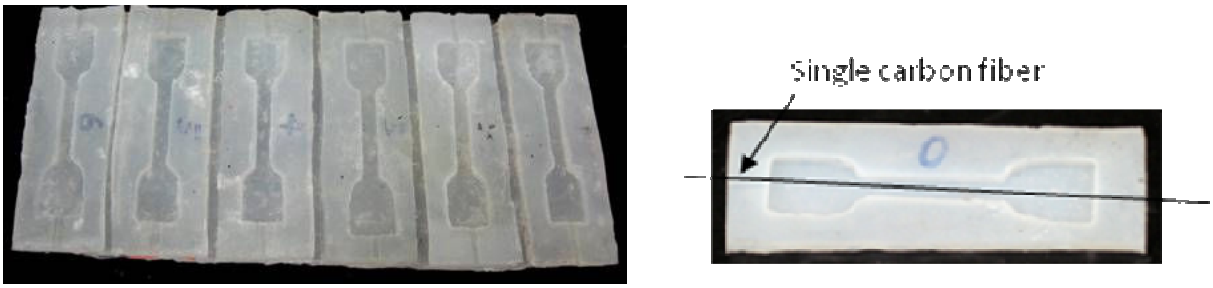

Figure 2.8 Silicon Rubber Forms (Molds) and Single-fiber Dog Bone Sample

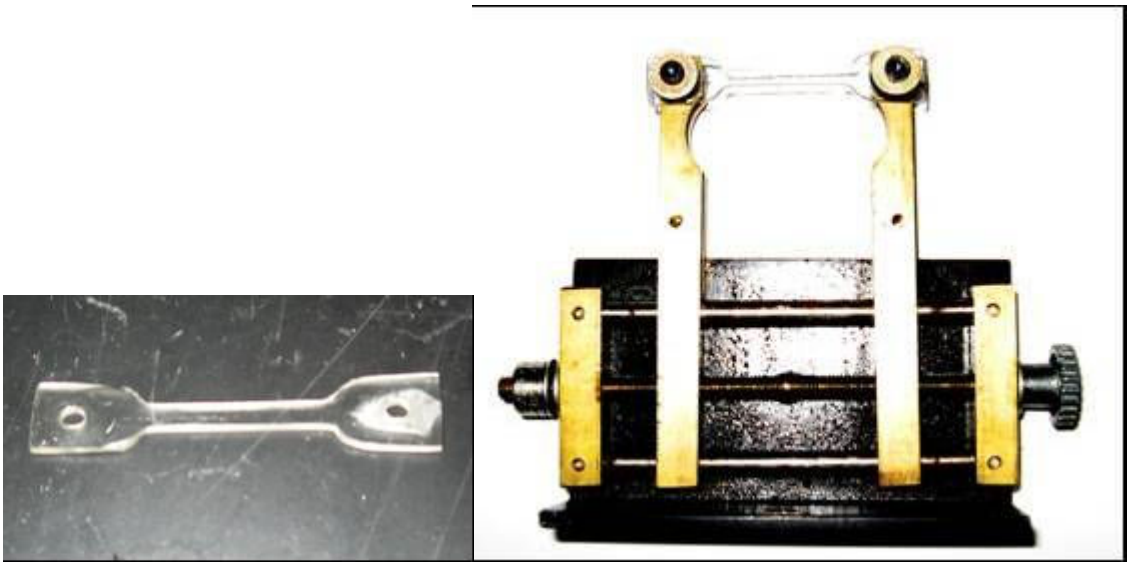

Figure 2.9 Specimen and Tensile Tester Apparatus.

Figure 2.10 Optical Microscope.

E: Apparent Density and Electrical Conductivity

A property of composites which merits attention is the apparent density and electrical resistance, because carbon fiber and matrix have different density and electrical resistance.

The tested samples are the same as the samples for tensile or flexural tests, but measured before the mechanical tests. Pre-cut carbon fiber composites coupons were sanded carefully which should be useful if the ends of the coupons need to be smoothed and leveled. This is important for making good measurement and good contact with the conductive clamps to the entire surface area at the ends of the samples. All coupons were dried in an oven at a temperature of approximately 150°C for overnight. After cooling for 5 minutes in a desecator, the samples were weighted with a balance. The dimensions of each sample were then measured with a calibrator. The apparent density (ρ) was calculated from above measurement.

$$\rho = \frac{\textbf{Mass (grams)}}{\textbf{Length (cm)} \times \textbf{width (cm)} \times \textbf{thickness (cm)}} \qquad (3)$$

For the measurement of electrical resistance, silver paint (spi # 5001 from SPI supplies, Inc) is used to coat the ends of the coupons. This makes the entire sample and its inner fibers one conductive bridge. A conductivity bridge was used to measure the resistance of the coupons. A conductive clamping apparatus was used to firmly make contacts between the ends of the samples. Alligator clamps were attached to the clamps to complete the circuit. A Model 31 Yellow Springs Instrument Conductivity Bridge was used to measure the electrical resistance of the coupons.

The conductivity bridge provided the resistance R of our material in Ω. Resistivity can be classically stated as the resistance within a surface area over some distance. We then use the equation:

$$P = \frac{Rdw}{l} \tag{4}$$

From above the resistivity is denoted ***P***. The variables ***d***, ***w***, and ***l*** will represent the thickness, width and length respectively. The units will be ohms centimeters (Ω cm).

F: Optical Microscope (Embed Sample)

Optical microscope testing evaluated fiber volume, orientation and distributions in the composites. Three rectangular bars, remnants of flexural or tensile testing, were placed in a cylindrical epoxy sample holder (see **Figure 2.11** (left)) with the fiber orientated at 0° and 90°. The samples cured and subsequently polished (see **Figure 2.11** (right)) for easy observation through optical microscope.

G: Scanning Electron Microscopy (SEM)

Scanning Electron Microscopy was done to produce high resolution images of sample surfaces. SEM testing is preferred over optical for its large depth of field and high resolution. This allows a large amount of sample to be in focus at one time. The closely spaced features can be examined at a high magnification and better judgment can be made on the quality of composite material. SEM allows us to easily view surface fractures and internal flaws and voids.

The SEM machine is a SUPER-III A, International Scientific Instruments. The data recorded was processed by EDS 2004 version 1.3 Rev P, IXRF system. Broken CFC samples are placed in a vacuum tube and electrons supplied from an electron gun whose beams are focused onto the surface and travels back and forth across the surface by alternating voltages in the scan coils. Scattered electrons are collected by a detector and produce images with 3-5 nm resolution, depending on the strength of the vacuum.

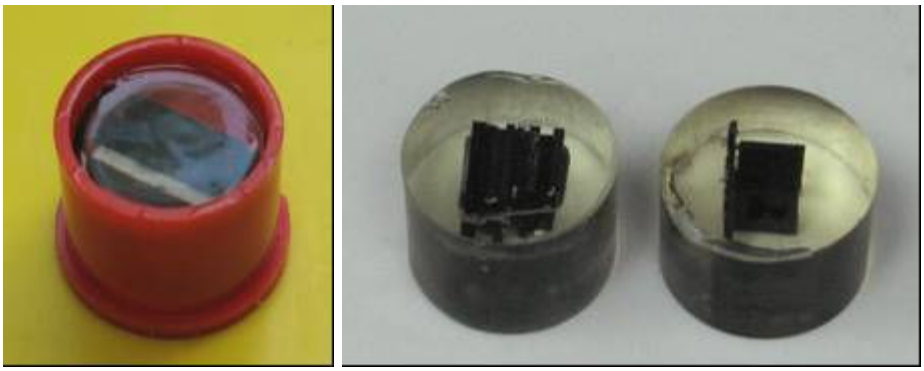

Figure 2.11 Embedded Carbon Fiber Composite Samples.

It should be noted that carbon fibers, although already conductive, can be coated with metals such as gold by sputter coating to give higher resolution samples. Typically this is a required step in processing samples as many materials are not conductive.

H: X-ray Diffraction

X-ray diffraction provides detailed information about the crystal structure of the carbon fibers. Carbon fibers were ground into a fine powder then impregnated with Vacuum grease to adhere it to a mold. Once in the mold the mixture is smoothed and leveled for good diffraction. The x-ray diffractometer used is a X'Pert –MPD system Philips Analytical X-ray PW 1700. The wavelengths of the X-rays emitted are 1.54 Angstroms. All samples were set to be scanned at angular position 2θ from 15 to 90 degrees. The rate at which the samples were scanned is 0.01 degrees per 2 seconds.

Chapter 3: Optimizing Process for Carbon Fiber Composite Fabrication.

The primary purpose of this task is to determine the best method to produce the highest quality carbon fiber composites from our low-cost carbon fibers. The composite samples are fabricated using continuous carbon fibers. Eventually these composites will be evaluated to determine various mechanical and electrical properties. The following sections describe the effect of various experimental fabrications on carbon fibers-reinforced composites.

Effect of Fabrication Techniques

As stated in Ref. [6], two fabrication techniques, vacuum bagging (VB) and vacuum bagging resin infusion (VBRI), have been widely accepted in the process of PAN-based carbon fiber (fabric)/resin composites. UTSI carbon fiber is roving-like pitch-based carbon fiber which form is totally different from the commercially available PAN-based carbon fibers (see **Figure 3.1**). Different formation of carbon fiber should require different fabrication techniques for the fiber composites. Therefore, at the beginning of the experiments, it is very important for us to find out the best fabrication techniques for making UTSI roving-like carbon fiber composites.

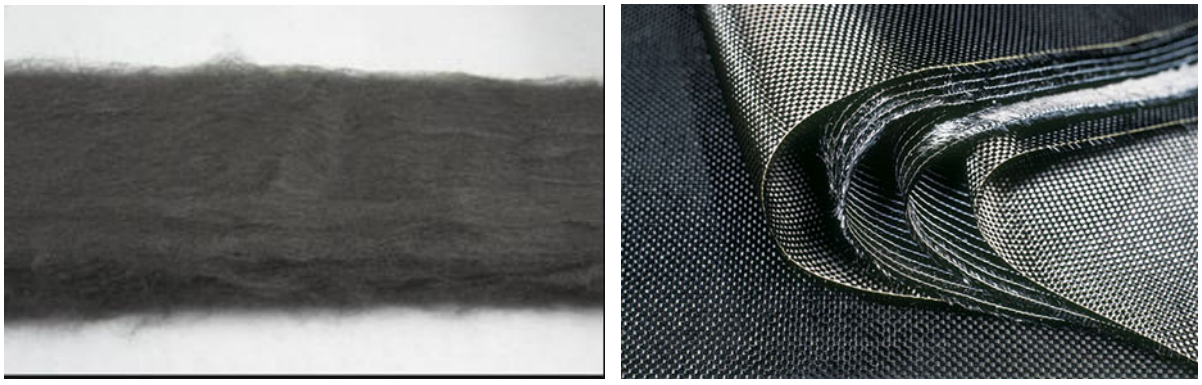

(A) (B)

Figure 3.1 Fiber Form Comparison between UTSI CF (A) and Commercial CF (B)

(A) Roving-like Pitch-based CF; (B) PAN-based Carbon Fiber Fabric.

To compare with two fabrication techniques, two composites were prepared with same UTSI carbon fiber, epoxy resin, and hardener (slow #206), but using different fabrication techniques. The two composites were measured for their apparent density, electrical resistivity, and tensile properties. The average data are listed in **Table 3.1**. The typical stress-strain curves for two composite's tensile tests are shown in **Figure 3.2.**

From **Table 3.1**, the composite prepared with VB shows higher carbon fiber content than the composite prepared with VBRI (just vacuum, without applying for pressure by press). This is because the breathe fabric used absorbed some extra resin during the VB process, therefore under the same pressure with VB, VBRI would keep more resin in the composite.

It is well known that the mechanical properties of carbon fiber composites increased with fiber volume in the composites [6]. As compared with VB- composite, VBRI-composite shows lower tensile modulus, higher ultimate strain and higher electrical resistivity due to its lower fiber content. The reason is that carbon fiber has extra high modulus and is more conductive than epoxy resin. However, VBRI-composite displays higher tensile strength. This is likely to be the result of lesser defects such as smaller porosity in VBRI composite. The evidence is its higher apparent density. Scanning Electron Microscopy (SEM) (see **Figure 3.3**) clearly shows more macropores existed in the VB composite than in the VBRI composite.

VB revealed evidence for improvement, made apparent by the methods lack of control in fiber volume, due to the forces that are attainable using only atmospheric pressure. The maximum pressure attainable using atmospheric pressure is 0.101Mpa. This pressure is not adequate enough to tightly pack fibers into the molding. The wetting method and curing process also lacks the ability to eliminate voids. Gaseous bubbles are not easily forced out by pressure differences. Poor control on surface pressure does not provide the composite with uniform thickness.

Table 3.1 Properties of Carbon Fiber Composites Prepared with Two Methods

Property (Average data)	Composite prepared with VB	Composite prepared with VBRI
CF content (wt %)	13-18	10-13
Apparent density (g/cm^3)	1.13	1.20
Electrical resistivity (Ω∗cm)	0.057	0.103
Tensile strength (Mpa)	75.95	84.37
Ultimate strain (%)	0.76	0.92
Young's modulus (Gpa)	9.8	8.9

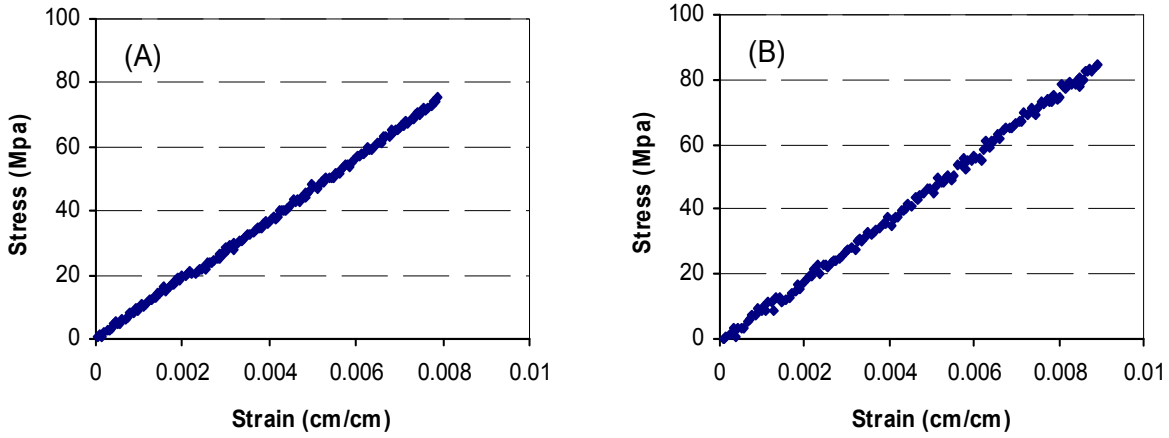

Figure 3.2 Typical Stress-strain Curves of Composite (A) Prepared with VB and Composite (B) Prepared with VBRI.

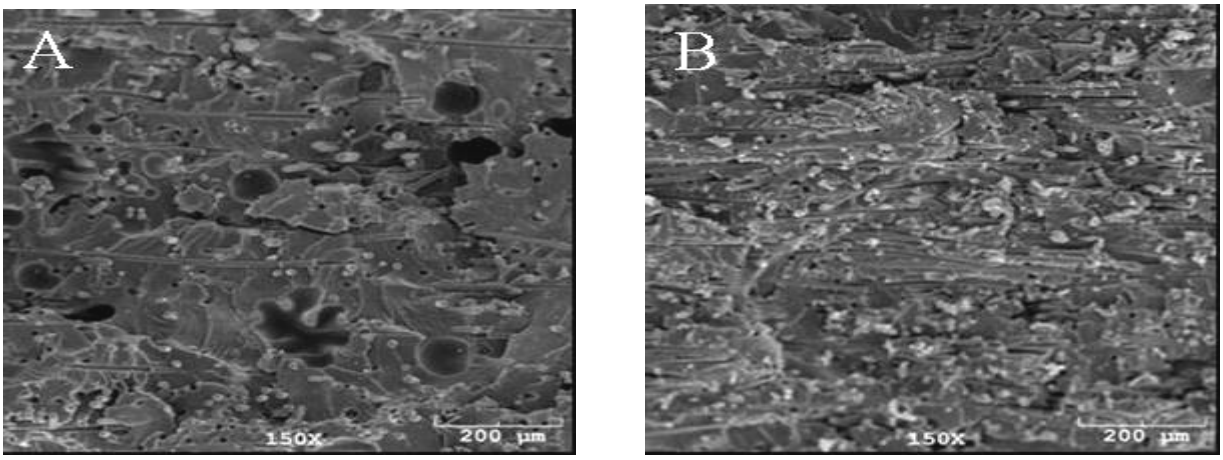

Figure 3.3 SEM Micrographs of VB-composite (A) and VBRI-composite (B)

The VBRI process demonstrated a better control of porosity while the pressures provided by the hot press provided good control of fiber volume and uniformity of thickness. Higher pressures may provide great fiber volume and uniformity of thickness.

From above experiments, it suggests that vacuum bagging resin infusion (VBRI) be a better technique for the fabrication of UTSI roving-like carbon fiber composite. Thus, VBRI process is the only process used in the following experiments.

Effect of Hardener

As indicated above, VBRI process provides an opportunity to increase fiber volume (content) by applying pressure (hot press) during the resin infusion process. However, it was found that the compressed fiber layer blocked the diffusion of resin and made a very long resin infusion time. Sometimes if the pressure is too high or the room temperature is relatively higher the resin will cure during the fabrication process without wetting all the fiber. Thus, to improve the VBRI process, an extra slow hardener (# 209) was employed to replace slow hardener (# 206). Two UTSI composites were prepared by using same carbon fiber and same VBRI fabrication process at a pressure of ~ 1 Mpa, but using different hardeners.

Table 3.2 lists the properties of the two composites prepared using two different hardeners. It can be seen that with a pressure used during the resin infusion, two VBRI composites show high fiber content at 20 - 26 wt%. Extra slow hardener # 209 displays a significant advantage over the hardener # 206. It was found that during the resin infusion, with extra slow hardener # 209, the composites can be prepared at a relatively high temperature of ~40^{o}C. This greatly decreases the viscosity of epoxy resin and shortens the fabrication process time. Furthermore, the composites made from slow hardener # 209 show higher apparent density, electrical conductivity, tensile strength and modulus.

From this experiment, it suggests that extra slow hardener # 209 is better than slow hardener # 206 for the used epoxy resin in the VBRI fabrication of UTSI carbon

fiber composites. Thus, extra slow hardener # 209 is only used with epoxy resin in the following study.

Table 3.2 Properties of Carbon Fiber Composites Prepared Using Two Different Hardeners (With A Pressure at ~1 Mpa).

Property (Average data)	Composite prepared with hardener 206	Composite prepared with hardener 209
CF content (wt %)	~ 20	~ 26
Apparent density (g/cm^3)	1.29	1.31
Electrical resistivity (Ω*cm)	0.109	0.032
Tensile strength (Mpa)	88.33	124.69
Ultimate strain (%)	0.66	0.88
Young's modulus (Gpa)	13.6	14.6

Effect of Pressure

Initial vacuum bagging demonstrated a need to better control carbon fiber volume. Generally it is a well known fact that the mechanical properties of PAN-based CFC are directly proportional to carbon fiber volume. To obtain higher fiber volume in UTSI composites a hot press was used in conjunction with the resin infusion process. Variable pressure can be applied during or after the infusion of resin. The affects of variable pressures on mechanical and various other physical properties will be determined at the end of this experiment.

UTSI roving-like carbon fiber lays with identical mechanical properties were used to fabricate CFC's. This ensures good statistical/comparable data points. In addition flexural tests instead of tensile tests were used to characterize the mechanical properties of the composites; the reason being that flexural tests need relatively small size specimens. Typically flexural tests provide the same tends as tensile tests so the effects on data should be negligible.

A: Fiber Content vs Flexural Properties

A hot press was used to correct complications discovered in the original vacuum bagging technique. It provided several advantages over simply using ambient pressures to compress the fibers and produce a mold. 1) It provides control over resin temperature during the wetting/diffusion process and during curing. 2) It provides much higher pressures than the 1 atmosphere of ambient pressure. 3) It provides uniform pressure.

Initial fabrication used an elevated pressure of 1 ton. The fabrication process was repeated several times with pressure being the only variant. Subsequent pressures of 2, 3, and 7 tons were used in independent composite fabrication runs. Samples for study were cut from each of these four CFCs and their results were compared.

By controlling the force applied by the hot press, the pressure was controlled and the fiber content within the CFC was regulated. There is a clear correlation between pressure and fiber content shown in **Figure 3.4**. While increasing the pressure, the fibers are compressed together and the excess resin is forced out. This experiment indicates that the UTSI roving-like carbon fiber can be compressed with a hot press during the VBRI processes to fabricate CFC with high fiber content. If no porosity existed in such CFCs, fiber volume will increase as well as fiber content.

Optical analysis (**Figure 3.5**) of the four composites revealed two important effects of applied pressure on the fiber content/volume and fiber morphologies. First, greater pressure increases the fiber content/volume by compressing the webbing. Pressure in excess of 3 tons more than doubles the fiber content. An increase in the number of fibers per area can clearly be seen in **Figure 3.5** C and D. Second, these graphs also show an increase in damage done to the fibers as a result of crushing. The optimal pressure for gaining maximum flexural strength, while avoiding damage to the fibers, was found to be 2 tons. Cracks created by higher pressures may serve as points of failure during flexural testing. The affects are reflected in the flexural strength vs.

pressure curve in **Figure 3.6**. The raw data for pressure effect are located in **Appendixes C, D, E, F.**

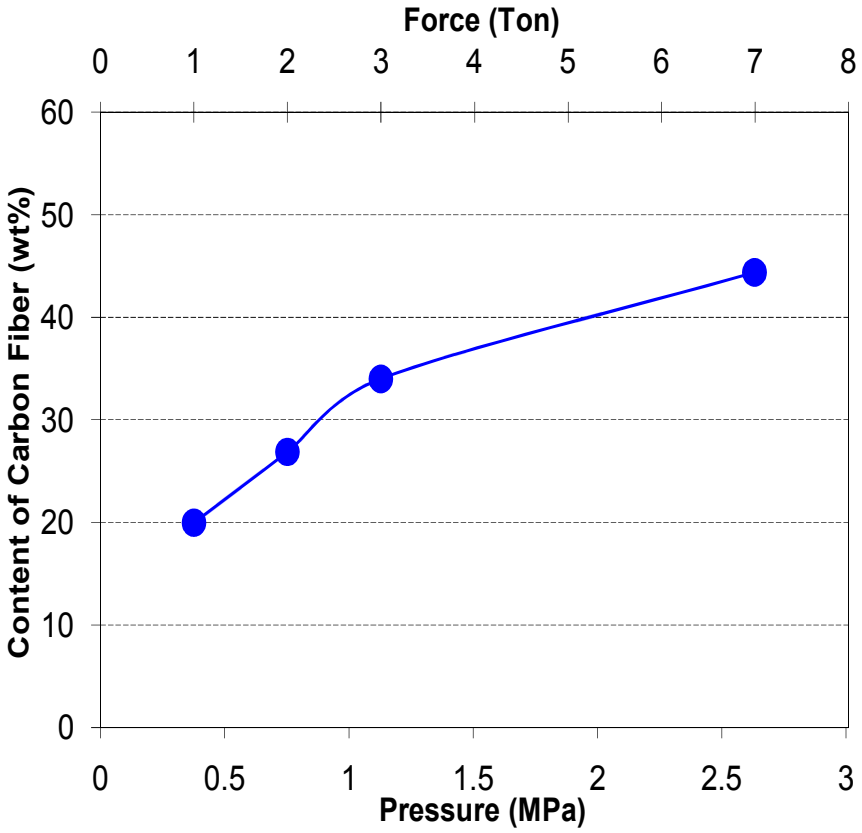

Figure 3.4 Effect of Applied Pressure on Carbon Fiber Content of the Composites.

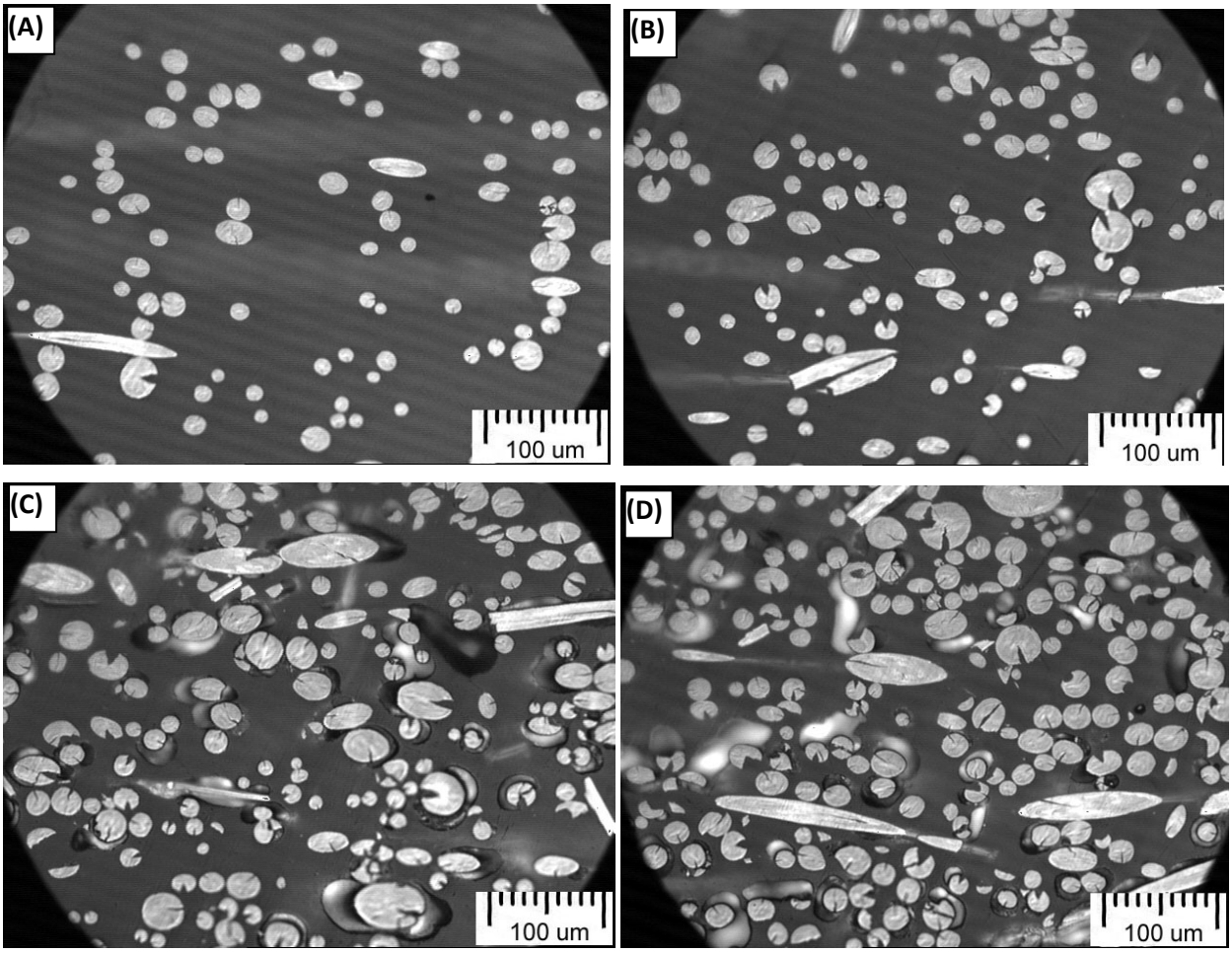

Figure 3.5 Typical Optical Microscopy Images of Carbon Fiber Cross-sections in Epoxy Resin Fabricated at Pressures (A): 1 Ton, (B) 2 Tons, (C) 3 Tons, and (D) 7 Tons.

Observation of **Figure 3.6** indicates the flexural modulus of the CFCs increased with increasingly applied pressure. This is expected due to the increasing carbon fiber content/volume within the composite as well as the fact that carbon fiber possesses a much higher modulus than cured epoxy resin. However, flexural strength only increases within the low pressure range (less 2 tons) but decrease at a higher pressure (3 tons) and then slowly increased with much higher pressures applied in this study. It was found from **Figure 3.4** and **Figure 3.5** that high pressure leads to not only high fiber content but also fiber cracking. High fiber content would increase the flexural strength while more fiber cracking decreases the strength.

This experiment suggests that UTSI roving-like carbon fiber can be compressed with a hot press to fabricate CFCs possessing high fiber content. For the carbon fibers studied in this section, the optimum range of applied pressure to produce CFC with the best flexural strength is around 0.75 MPa (or ~2 tons in force for the tested model). Pressures beyond this will contribute high modulus but will not show obvious help in increasing flexural strength due to fiber cracking.

B: Fiber Content vs Apparent Density

Apparent density is one of key parameters to be controlled in the fabrication of carbon fiber/resin composites. Its value reflects the ratio of carbon fiber (the density of UTSI carbon fiber is estimated at 1.5 -1.7 g/cm^3 due to low carbonization temperature) to the resin (the density of cured epoxy is ~ 1.20 g/cm^3) and porosity in the composite does so as well. In this study, composite volume and weight measurements were taken before each flexural test. Within these measurements composites fabricated at different pressures were compared in order to understand the effects of pressure on apparent density as shown in **Figure 3.7**.

It should be expected that all the composites will display higher apparent densities than the cured epoxy resin (~ 1.20 g/cm^3) fabricated without applied pressure. Apparent density increased with increasing pressure below the range of 1.13 Mpa (3 tons). The

apparent density increased with increasing pressure, simply because applied pressures forced out excess resin and tightly pack fibers which leads to an increase in the ratio of carbon fiber to resin in the composite.

However, low apparent density appeared when the applied pressure was too high. The most probably reasons being the following: 1) too much pressure crushes the fibers and forces out not only excess resin but also powdered fibers; 2) too much pressure also traps gaseous pockets and slows the diffusion process to such a degree that these pockets do not have sufficient time to escape the inner most core of the composite material. These effects lead to an overall loss in apparent density. The results also reveal that a high porosity exists in composites made under very high pressures.

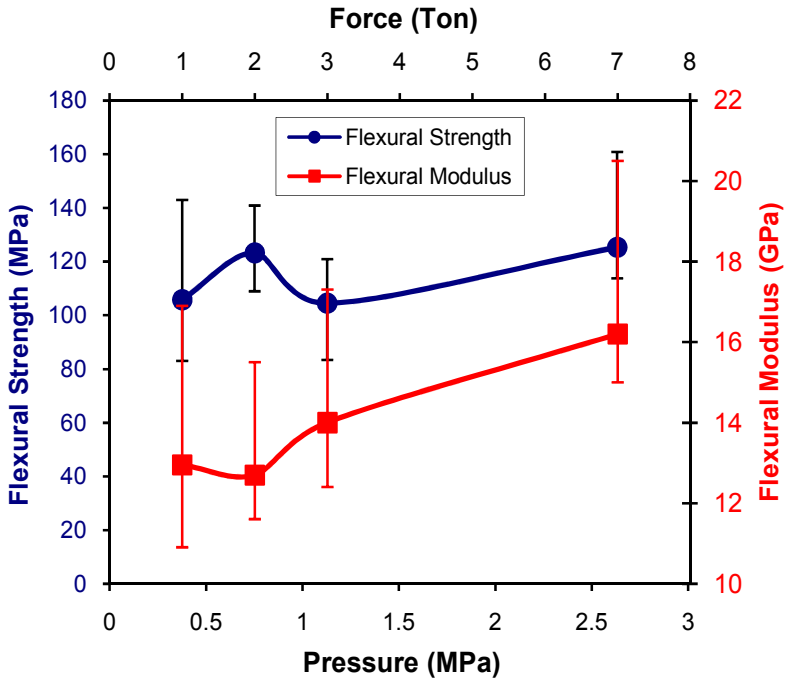

Figure 3.6 Effect of Applied Pressure on the Flexural Strength and Modulus of the Composites.

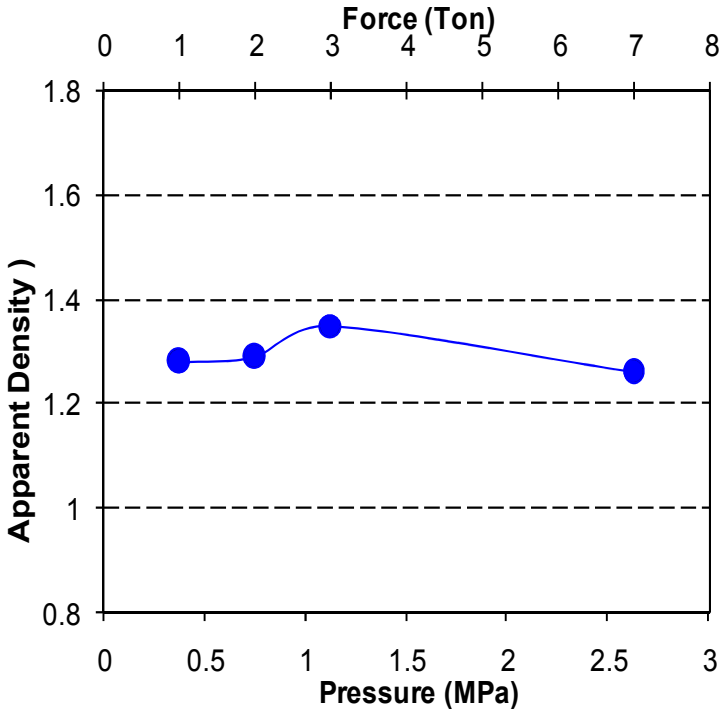

Figure 3.7 Effect of Applied Pressure on Apparent Density of the Composites.

C: Fiber Content vs Electrical Resistivity

Applied pressure during the curing process directly affects the electrical conductivity (**Figure 3.8)** of CFCs. It must be noted that there are many factors that could affect the resistance of a composite. Many of these variables are manifested within the fibers themselves such as fiber electrical resistivity, continuous or short fiber, uniformity of diameter, cross sectional shape, and various treatments. It is hoped that through enough collection of data a conclusion can be made as to what degree conductivity determines the quality of carbon fiber composites.

The level of conductivity for each sample was determined by measuring its resistivity as shown in **Figure 3.8**. Resistivity is resistance within a surface area over some distance. The overall relationship between volume and electrical conductivity was found to be linear since the relationship between the fiber volume and resistivity is inversely proportional. This was expected since the carbon fibers are conductive; hence, higher volumes yield lower resistivity. High pressure not only provides high content of carbon fiber but also makes high contact efficiency among the individual fibers even crushed fibers in the composites.

In the case of the pressure at 1.13 Mpa (3 tons), it shows a high resistivity (or low conductivity) though it has higher fiber content than the CFCs made at a lower pressure. The reason for this is likely to be that the carbon fibers were crushed by the pressure creating gaps along the fiber length. This effectively turns the continuous fibers into short fibers. These short fibers were unable to complete the bridge (bad contact among the fibers) due to a lack of enough pressure to provide high contact efficiency and would not let current travel from one end of the sample to the other.

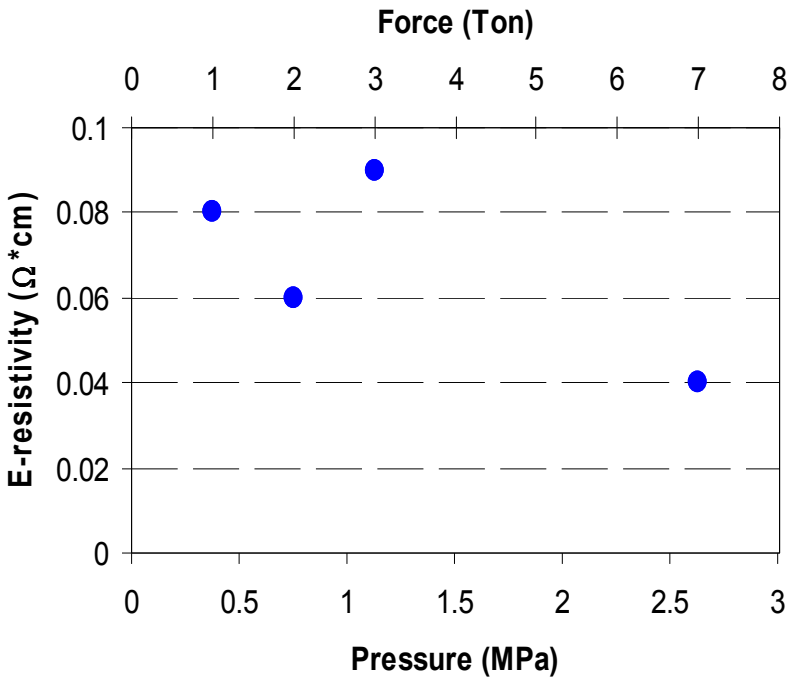

Figure 3.8 Effect of Applied Pressure on Electrical Resistivity of the Composites.

Effect of Matrix

In order to further determine the fabrication process for UTSI carbon fiber composite, different matrix materials were used in this study for comparison. Initial UTSI CFCs were prepared using epoxy resin, because the mechanical properties of epoxy resin and its composites are generally very good. However, epoxy resin has relatively high cost and relatively poor heat resistance as compared with phenolic resin. It is common knowledge that phenolic resin composites can also be converted into carbon-carbon composites which are highly heat resistant and great for application in thermally protective materials that are also wear resistant. In order to determine what kind fabrication process is suitable for making UTSI phenolic resin composites and carbon/carbon composites preliminary work has been done to explore the fabrication of such new composites with the UTSI roving-like carbon fibers.

A: Phenolic Resin Composites

H. Hatta and K. Goto described composites with a phenolic matrix as having an inherent risk of trapping gases expelled by the solvents during the curing process [4]. In order to ensure these solvents evaporate from the phenolic resin the temperature of the hot press must be raised to 100°C. In this study, CFC's with phenolic matrix materials were fabricated with and without degassing process to study the treatments affect on the porosity (see **Figure 3.9**), apparent density, resistivity, and flexural properties as shown in **Figure 3.10** and **Figure 3.11**. The raw data for phenolic resin composites are located in **Appendixes G** and **H.**

Without the Degas process, composite apparent densities were slightly below 1 g/cm^3. Subsequent investigation using an optical microscope confirmed the presence of large amounts of voids (**Figure 3.9**a). These voids are the direct cause of significantly lower apparent densities. With degassing, phenolic CFCs reached apparent densities as high as 1.3 g/cm^3. The Degas process eliminates the vapors emitted from the solvents during curing and therefore allows room for more matrix material. The absence of gaseous voids was optically confirmed in **Figure 3.9** b.

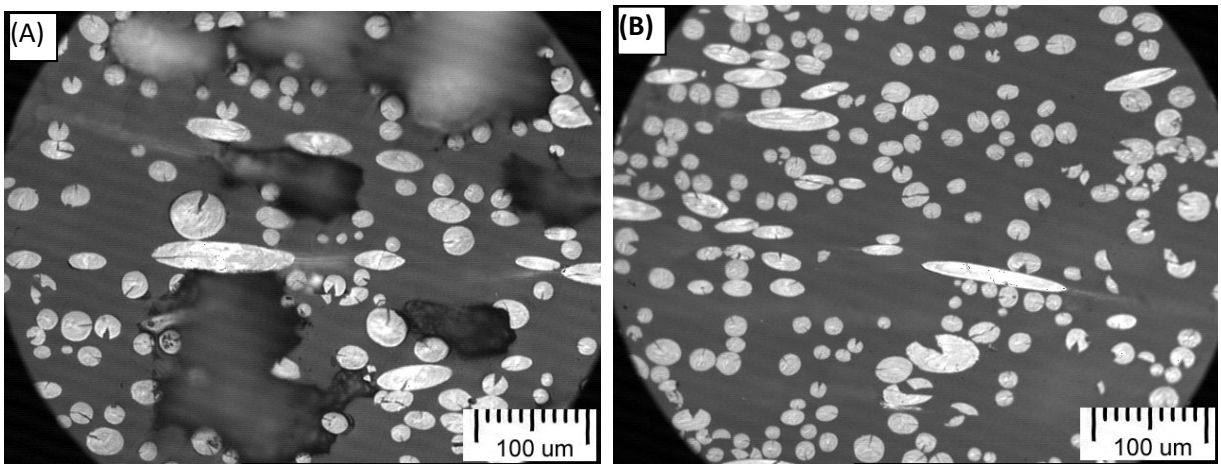

Figure 3.9 Typical Optical Microscopy Images of Phenolic Resin /Carbon Fiber Composites Fabricated with Two Different Processes. (A) Without Degas Process, and (B) With Degas Process.

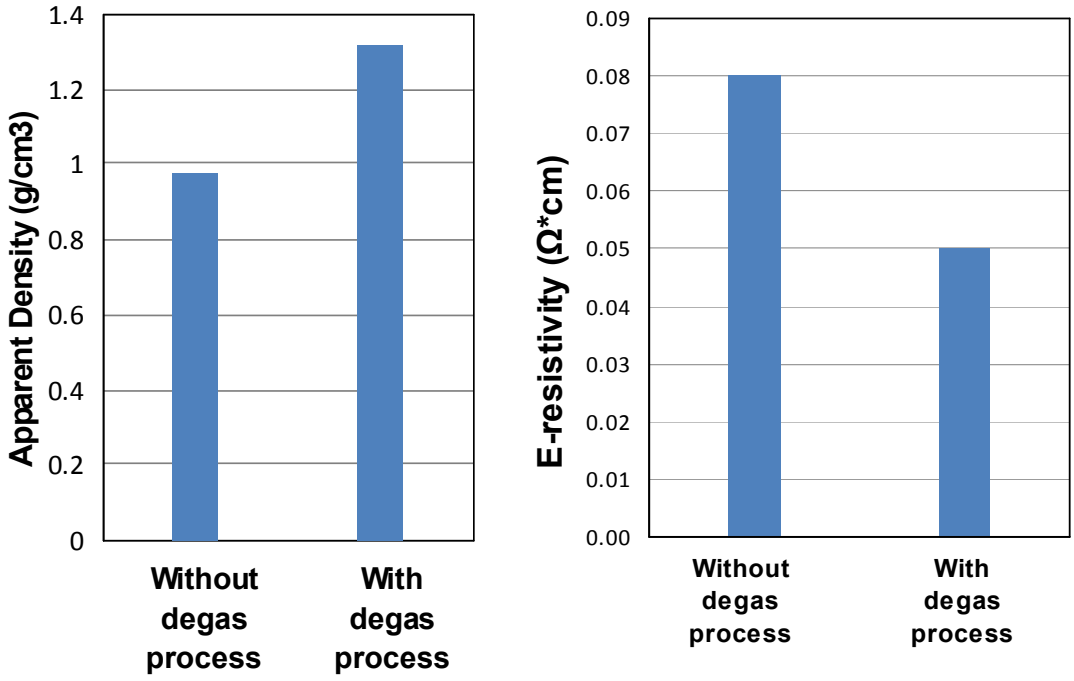

Figure 3.10 Effect of Degas during Fabrication Process on Electrical Resistivity and Apparent Density of the Carbon Fiber/Phenolic Resin Composites.

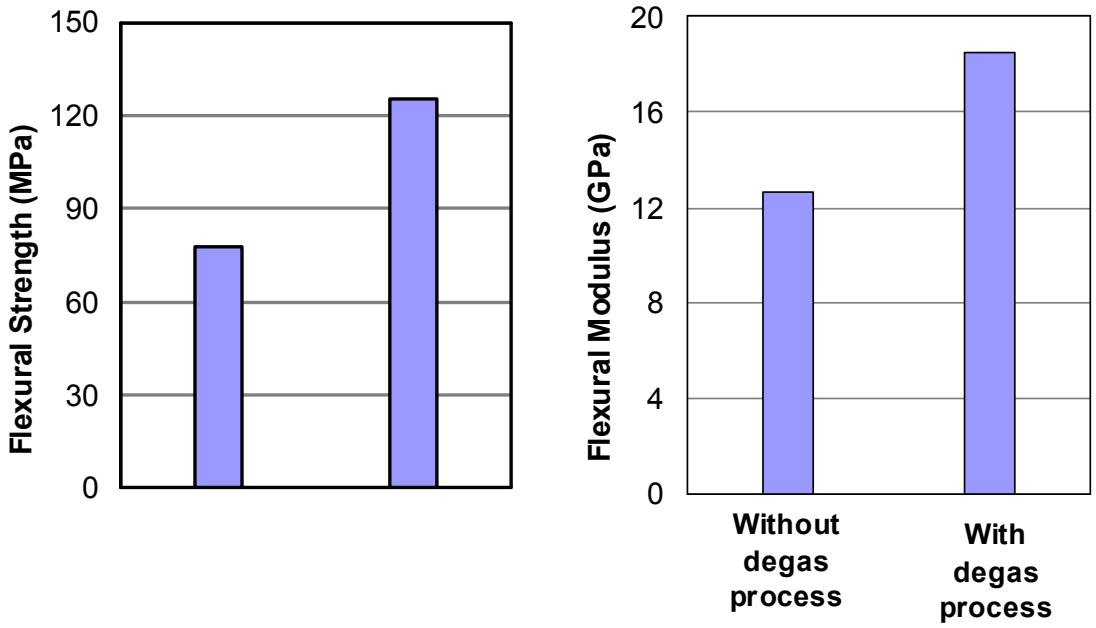

Figure 3.11 Effect of Degas during Fabrication Process on the Flexural Strength and Modulus of the Carbon Fiber/Phenolic Resin Composites.

Without the degas process resistivity reached 0.08 Ω*cm. The presence of voids caused by expanding gases decreased the concentration of carbon fibers lowering carbon fiber volume. With the degas process carbon fiber composites becomes less resistive. It reached resistivities as low as 0.05 Ω*cm. The degas process increases carbon fiber content and therefore conductivity.

Flexural testing also confirmed expected effect of degas on the void content and mechanical properties. The composite with fewer voids possess superior mechanical properties over the composites with more voids. Composites tested without the degas process have flexural strengths of approximately 75 MPa and a flexural modulus of just over 12 GPa. Degas treatment improved the mechanical properties, obtaining flexural strengths of over 120 MPa and flexural modulus of over 17 GPa.

Our investigation into phenolic resin/carbon fiber composites suggest that degassing is essential in creating high quality CFC's. Degassing decreases voids, and increases apparent density, electrical conductivity, and flexural strength and modulus.

B: Carbon-carbon Composites

Phenolic resin composites were also converted into C/C composites as shown in **Figure 3.12**. The goal of this investigation is to explore the changes in physical properties from a phenolic resin composite to a C/C composite.

In this study, the phenolic resin CFC prepared with degas process was heated at 1100°C in N_2 to carbonize the matrix material. Once the carbonization is completed conductive properties, apparent density and flexural properties were evaluated. These results are shown in **Figure 3.13** and **Figure 3.14**. The raw data for this study are located in **Appendixes H** and **I**.

Apparent density (**Figure 3.13**) was investigated both before and after carbonization. Phenolic resin composite attained an apparent density of 1.3 g/cm^3. Carbon-carbon composites revealed much lower densities of little more than 0.9 g/cm^3. As the composite matrix is carbonized the phenolic resin decomposed and all non-

carbon elements were eliminated. The result of this process is a loss of weight and the formation of voids which can be seen in **Figure 3.12** b.

Conductive properties of these composites before and after carbonization were also compared in **Figure 3.13**. Prior to carbonization resistivity of phenolic CFC are 0.05 Ω*cm. After carbonization, the resistivity significantly decreased to 0.02 Ω*cm. This is expectable because carbon is highly conductive so composites will be highly conductive if both the fiber and the matrix material are carbon. Carbon matrix was confirmed in optical investigations and shows obviously brighter reflected light than cured phenolic resin as shown in **Figure 3.12**.

Flexural strength and modulus (**Figure 3.14**) are also decreased as a result of carbonization. Prior to treatment flexural strength is over 120 MPa. Flexural Modulus is over 18 GPa. After carbonization they decrease to ~ 30 MPa and ~ 8 GPa respectively. Carbonization of phenolic matrix results in many voids and defects to serve as points of failure during loads and stresses. However, it is believed that by employing several cycles of phenolic resin infiltration and carbonization, the C/C composites will demonstrate much higher apparent density and better flexural properties.

Our study determined carbon-carbon composites to be easily prepared from phenolic resin/UTSI carbon fiber composites. The carbonization of phenolic resin matrix reduces the apparent density and also creates many defects due to the decay of non carbon elements. These massive amounts of defects also serve as the key source for reducing the mechanical properties of the C/C composites.

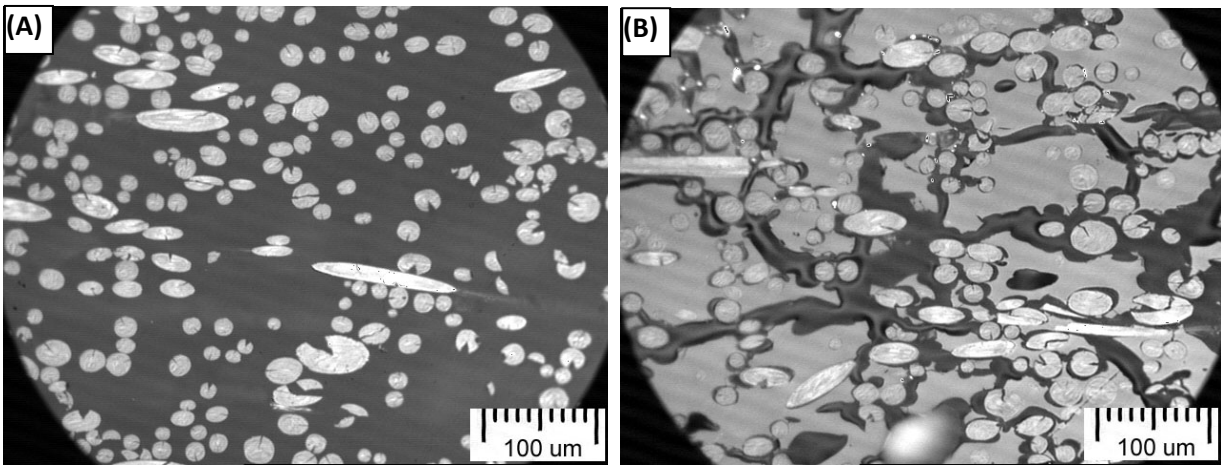

Figure 3.12 Typical Optical Microscopy Images Showing a Conversation from (A) Phenolic Resin Composite to (B) Carbon-carbon Composite.

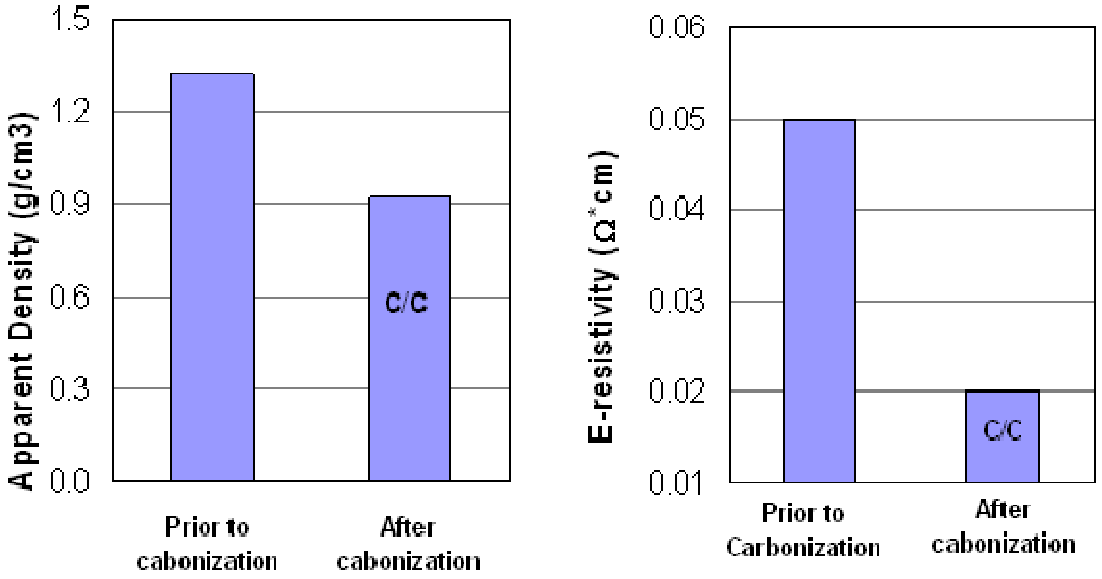

Figure 3.13 Changes in E-Resistivity and Apparent Density As a Phenolic Resin/Carbon Fiber Composite Is Converted to a Carbon/Carbon Fiber Composite after Carbonization at 1000°C in N_2.

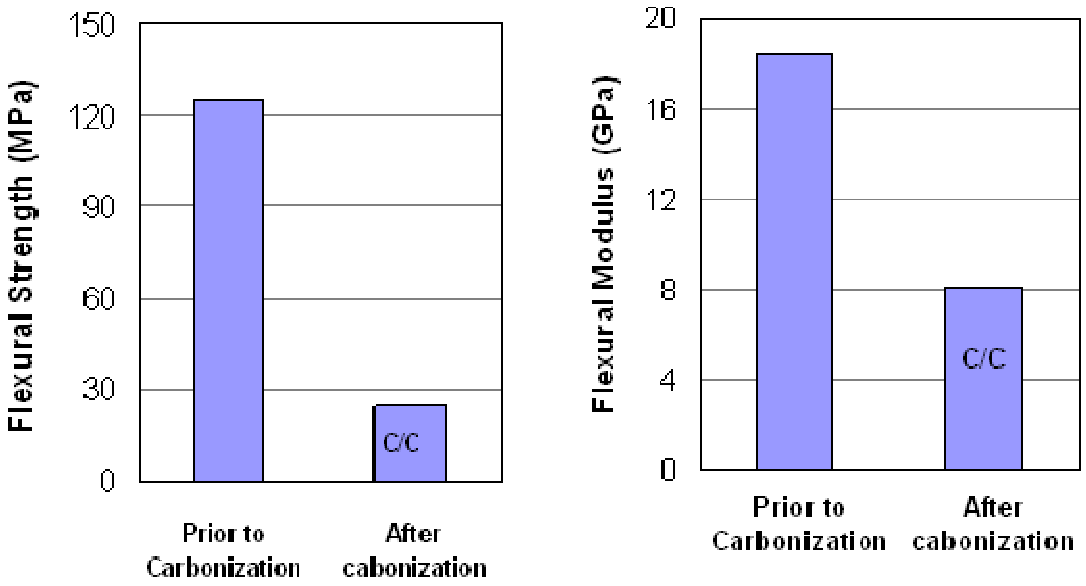

Figure 3.14 Changes in Flexural Strength and Modulus As a Phenolic Resin/Carbon Fiber Composite Is Converted to a Carbon/Carbon Fiber Composite after Carbonization at 1000°C in N_2.

Structure-property Analysis

Detailed characterization was undertaken to determine the means by which fabrication techniques affected the mechanical and other physical properties of UTSI CFC's. The goal of this research was to simply observe the internal structure of CFC's and quantify what changes occurred to the fiber and or matrix that led to the mechanical properties observed during flexural testing.

A: SEM

Infusion carbon fiber composite composed of UTSI carbon fibers and epoxy resin were first tensile tested; afterwards their fracture surface were analyzed by SEM as shown in **Figure 3.15**. It was found that carbon fibers were embedded in cured epoxy resin without significant air bubbles and voids on the overall surface. However, **Figure 3.15** (A) shows some fibers pulled out during tension leaving holes on the fracture surface. Closer inspection in **Figure 3.15** (B) clearly reveals deboning area between the fiber and the matrix material. This implies a problem between the bonding of the fiber surface and the epoxy resin. The results of SEM analysis demonstrated a need for a better CFC fabrication method. Poor bonding should be a result of low interfacial shear strength between fibers and epoxy resin.

B: Fiber X-ray Diffraction

To better understand the mechanism by which UTSI carbon fibers bond badly with epoxy resin, X-ray diffraction was employed to analyze the crystalline structure of the carbon fiber.

It is well known that commercially available type I carbon fibers possess a high modulus but also have a very inert surface [7], due to its perfect graphite-like crystal structure which results from very high temperatures (> 2000^{o}C) during the carbonization (graphitization) treatment. UTSI carbon fibers were converted from mesophase pitch fibers. As a result, the carbon fiber may be composed of graphite-like crystals though the carbonization temperature was as low as ~ 1050^{o}C.

To confirm this, two types of pitch fibers named mesophase and isotropic pitch fibers and their carbonized (1050^{o}C) fibers were tested using a X'Pert – MPD system Philips Analytical x-ray with a copper tube to emit x-rays at wavelengths of 1.54 Angstroms. The results are shown in **Figure 3.16** and **Figure 3.17**.

As expected mesophase pitch is different from isotropic pitch fiber. **Figure 3.16** reveals that mesophase pitch fibers posses an obvious peak at $2\theta = 25^{o}$ which may be associated with a crystalline structure in the mesophase pitch.

After carbonization at 1050^{o}C in N_2, the mesophase pitch-based carbon fibers developed a higher and sharper peak at the same position ($2\theta = 25^{o}$) as shown in **Figure 3.17**. The crystal size can be determined by the ***Scherrer equation*** [11],

$$\mathbf{Lc} = \mathbf{K}\,\boldsymbol{\lambda} / (\boldsymbol{\beta}\cos\boldsymbol{\theta}) \qquad (5)$$

where: **K** = shape factor (constant) ≅ 0.89 for Lc; **λ** = radiation wavelength (Å) = 1.54056 Å for copper Kα1; **β** = line broadening (value must be in radians); **θ** = Bragg angle (at maximum peak intensity).

From this equation, a sharper or narrower peak presents larger crystalline structures. This means that carbonization even at a low temperature of only 1050^{o}C greatly increases the size of the crystal originally presented in the mesophase pitch.

In conclusion, x-ray analysis demonstrated that carbonization at 1050°C provides the UTSI mesophase pitch-based carbon fibers with obvious crystalline structure. Thus The UTSI carbon fiber is most likely to have an inert surface making it difficult to bond with polymer resin during the fabrication of composites. In order to improve surface bonding, chemical reactivity of carbon fibers, surface treatment is essential.

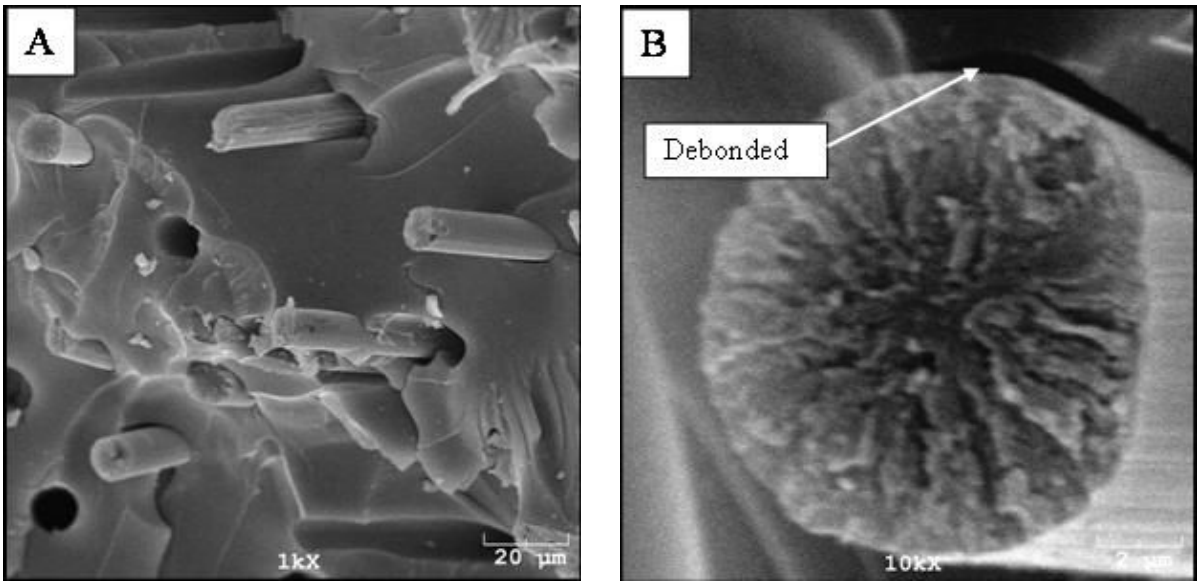

Figure 3.15 SEM Micrograph of Fracture Surface of UTSI CFC.

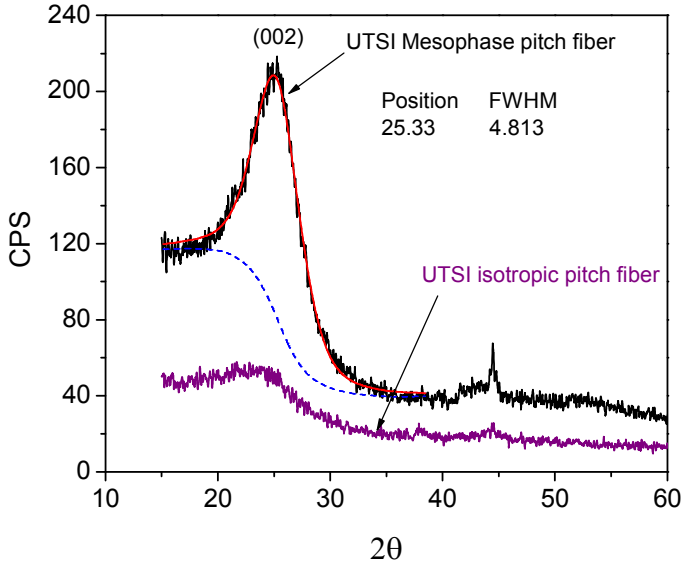

Figure 3.16 X-ray Diffraction Patterns of Mesophase and Isotropic Pitch Fibers.

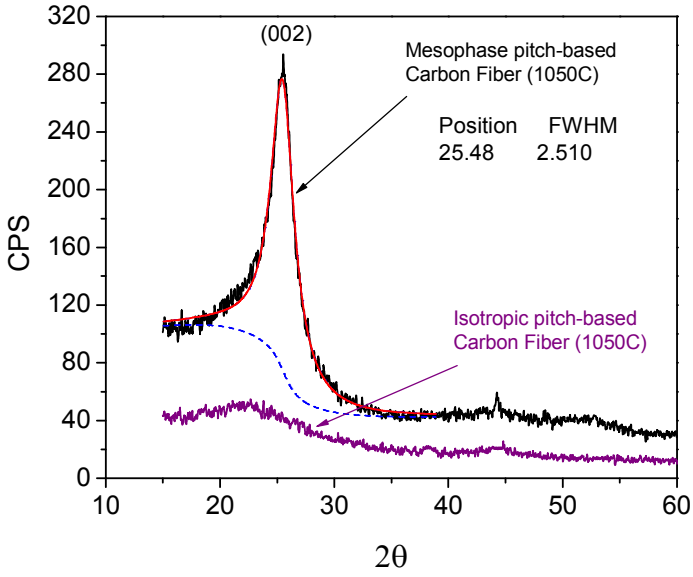

Figure 3.17 X-ray Diffraction Patterns of Mesophase and Isotropic Pitch–based Carbon Fibers.

Chapter 4: Surface Treatments for Improving Mechanical Properties of CFC

Chapter 3 demonstrated the ability to improve mechanical and other physical properties of UTSI CFC by optimizing the fabrication process through careful use of molding, matrix, hardeners and applied pressure. However, it was also found that bad bonding existed between the carbon fiber surface and the epoxy resin matrix due to the inert property of the as-received carbon fiber surface. An inert surface negatively influences the mechanical properties of the composite. To address this problem, fiber surface modification/treatments were performed in our laboratory to further improve the mechanical properties of UTSI carbon fiber composites.

The objective of this section is the study of how oxidative surface treatments strengthen the bond between carbon fiber and epoxy resin. By maximizing the bonding strength it is hoped that the mechanical properties of UTSI CFCs are improved as well. Currently there are several carbon fiber surface treatments for enhancing bonding between the fiber and matrix. These include gaseous oxidation, liquid phase oxidation, plasmas, whiskerization, polymer grafting, and coating to modify fiber surfaces. In this study, we will focus on gaseous oxidation with ozone, because it has the following advantages over other methods:

- Relatively low cost;
- Comparatively lower temperature required compared with air oxidation (>380^{o}C);
- Ease of operation and control in line;
- No chemicals required;
- No washing and drying processes as compared liquid oxidation;
- Uniform reaction between gas and fiber; in particular for the roving-like UTSI carbon fiber as compared with PAN-based tow form carbon fiber (compare the two carbon fiber forms in **Figure 3.1**).

To investigate the efficiency of ozone oxidation, as a comparison, concentrated HNO_3 solution was employed to treat the same fibers Ref. [6]. The latter was a very conventional method and considered to be very effective to enhance the concentration of fiber surface oxygen-containing groups and to greatly improve the degree of adhesion between the carbon fiber and resin.

Single-fiber Fragmentation Tests

This research involved treating UTSI carbon fibers with ozone at 150°C and with HNO_3 solution at 25 and 100°C, respectively. The parameters will be temperature and treatment time, altered with each test run in order to study how these treatments affect the fibers' mechanical properties. However, the main goal of these treatments was to introduce functional groups such as carboxylic acid which can react with hydroxyl groups in resin to improve the bonding between the fiber and matrix. In order to better understand the changes in the fibers surface properties, a single fiber fragmentation technique was used to characterize the bonding behavior in the interface between fiber surface and the matrix.

A: Fiber Fragment and Interface Patterns

As indicated in Chapter 2, single fiber/epoxy resin dog bone specimens were placed into a stretching apparatus where fragmentation tests were done under an optical microscope. Fiber fragmentation points were counted in order to determine fiber critical length and interfacial shear strength while the Interface patterns were observed with increasing applied strain on the specimen. Typical fiber fragment and interface patterns in the fiber/epoxy system can be observed in **Figure 4.1**. Image (A) is visible under normal light while the image (B) is shown with cross polarized light. Using polarized light enables crystallization and fragmentation to become clearly visible by causing light to filter through in specific colors and patterns. These patterns allow us to determine critical length and if the breaks are cracks or slips in the matrix as shown in **Figure 4.2**; also whether or not debonding occurs in the interface (**Figure 4.3**). Slips and debonding indicate poor adhesive between the fiber and resin.

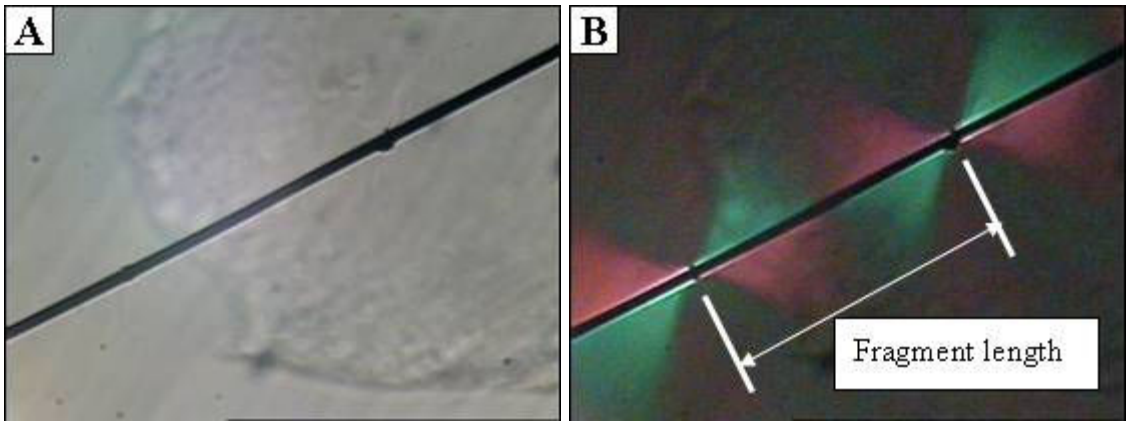

Figure 4.1 Typical Fragmentation Characterization for Carbon Fiber /Epoxy System. (A) Normal Light; (B) Cross-polarized Light.

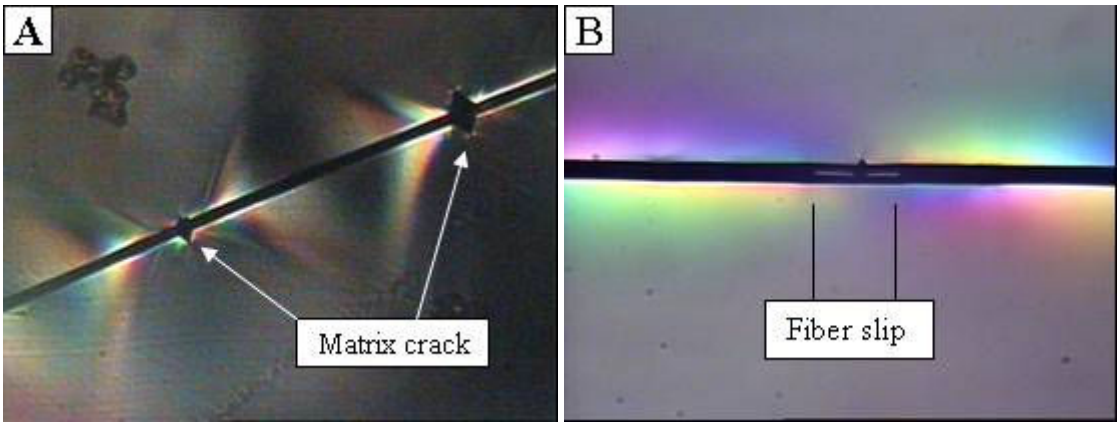

Figure 4.2 Interface Patterns for Carbon Fiber /Epoxy System. (A) Crack with a Deformation into Matrix; (B) Carbon Fiber Slip in the Matrix.

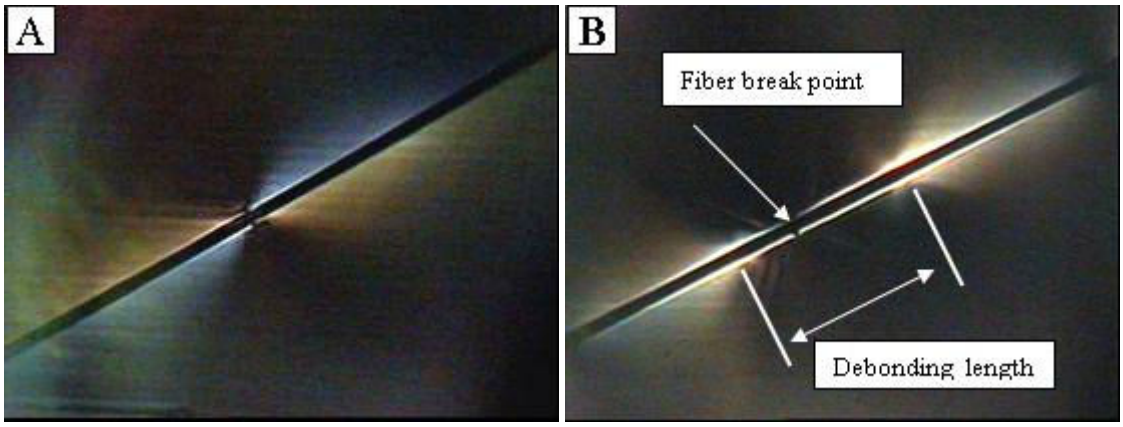

Figure 4.3 Interface Patterns for Carbon Fiber /Epoxy System. (A) Low Strain Applied; (B) High Strain Applied.

The effects of surface treatments on the interface patterns created during fragmentation testing are shown in **Figure 4.4**, which also compares the four UTSI carbon fibers 1) the as-received; 2) O_3 treated at 150°C for 30 min, 3) HNO_3treated at 25°C for 30 min, and 4) HNO_3 treated at ~ 100°C for 30 min. It can clearly be seen that all surface treated carbon fibers have a greater number of broken points (shorter average length) than the as-received carbon fibers. For the treatment with HNO_3, the high temperature gives shorter length than room temperature. Usually, if carbon fibers have identical diameter and tensile strengths, a shorter fragment length in one and not the other means the ladder possesses good adhesiveness in the interface between fiber surface and matrix. Statistical values for fiber average length along with fiber diameter and tensile strength are listed in **Table 4.1**. The raw data are enclosed as **Appendix J**.

B: Critical Length and IFSS

Single fiber fragmentation testing is used to determine the fiber critical length and interfacial shear strength or IFSS. The interfacial shear strength, τ, can be calculated with the following relationship [5]:

$$\tau = \frac{S_f \times d}{2 \times l_c} \qquad (6)$$

Where S_f is the fiber strength as evaluated from single fiber tensile tests, d is the fiber diameter and l_c is the critical fragment length of the fiber. The relationship between the critical length l_c and the average fragment length $\bar{l}$ is as follows.

$$l_c = \frac{4}{3} \times \bar{l} \qquad (7)$$

The average fragment length was calculated by dividing the initial whole accounted length of the fiber by the number of broken points plus one, n+1.

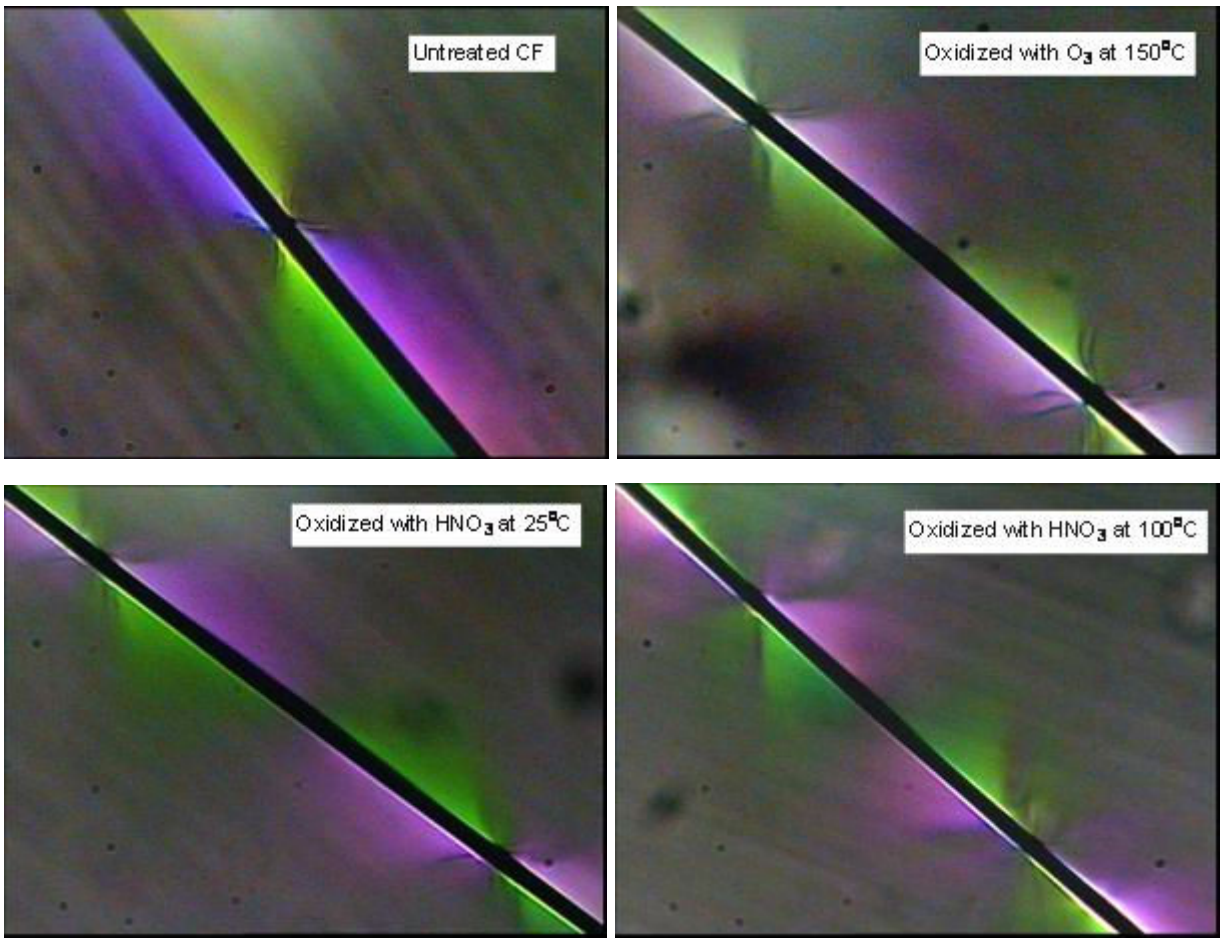

Figure 4.4 Typical Fragment Length and Interface Patterns for Four Different Carbon Fibers in the Epoxy Resin.

Table 4.1 summarizes and compares results for various critical length and shear strength of treated and untreated fibers. Analysis has shown an increase in interfacial shear strength (IFSS) in the system of carbon fiber upon oxidation. The increase in IFSS indicates an improvement in carbon fiber surface properties, such as higher surface area and more surface functional groups, which improve the wetting of the carbon fiber surface and the bonding with epoxy resin. It seems that O_3 oxidation is better than HNO_3 for the surface modification of the UTSI carbon fibers.

Table 4.1 Fragmentation Test Results for Surface Treated and Untreated Carbon Fibers.

Fiber Type	Fiber Diameter (μm)	Tensile Strength (Mpa)	Average length (μm)	Critical Length (μm)	IFSS (Mpa)
As-received UTSI CF1	12.46	464.95	491	654.5	4.4
As-received UTSI CF2	19.95	723.1	724	965.3	7.4
O_3 (150^{o}C) treated CF	19.15	706.3	450	600.0	11.3
HNO_3 (100^{o}C) treated CF	19.05	884.0	596	794.7	10.6

Composite Property Tests

Single fiber fragmentation tests showed that HNO_3 and O_3 treated carbon fibers have higher IFSS than as-received carbon fibers in the epoxy resin system. To better understand the effect of surface treatment on the surface properties a comparative study was conducted in real carbon fiber composites.

UTSI carbon fiber L00085-86 was employed in this study and treated with HNO_3 or O_3 respectively. The fibers prior to and after surface treatment were fabricated to composite plates with epoxy resin under same conditions. Their apparent density and electrical resistivity are shown in **Figure 4.5**. The raw data for this study are located in **Appendixes E, K,** and **L**.

It can be seen that apparent density does not change with surface treatment, but electrical resistivity appears to be increased after surface treatments. The probable reason is more surface functional groups not only increased bonding between fiber surface and epoxy resin, but also increased the surface electrical resistance of the carbon fiber and further increased the contact e-resistance among the filaments in the composites.

The flexural strength and modulus of three composites are shown in **Figure 4.6**. Fiber surface treatments greatly increased both strength and modulus of the composites as compared with untreated carbon fiber. Additionally, O_3 treatment better improved the flexural properties of UTSI CFC than HNO_3 treatment.

Typical optical microscopy images of the three composites are shown in **Figure 4.7**. It appears that the debonding area around each fiber greatly decreased from untreated fiber (A) to surface treated fibers (B) and (C). This strongly suggests that fiber surface treatments increase the wettability of the fiber surface, leading to better bonding between carbon fiber surface and epoxy resin.

In conclusion, fiber surface treatment is a very important process for producing high performance composites from UTSI mesophase pitch-based carbon fibers. Surface treatment with O_3 proved to be the most effective for UTSI carbon fibers.

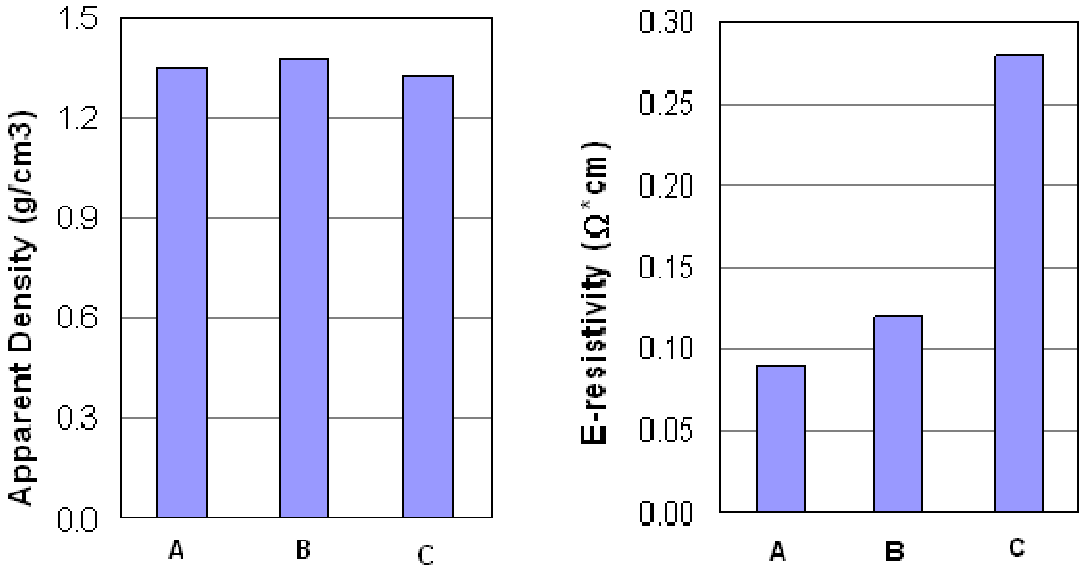

Figure 4.5 Effect of Fiber Surface Treatments on Apparent Density and Electrical Resistivity of the Carbon Fiber/Epoxy Composites.

A: As-received; **B**: HNO_3 Treated; and **C**: O_3 Treated Carbon Fibers.

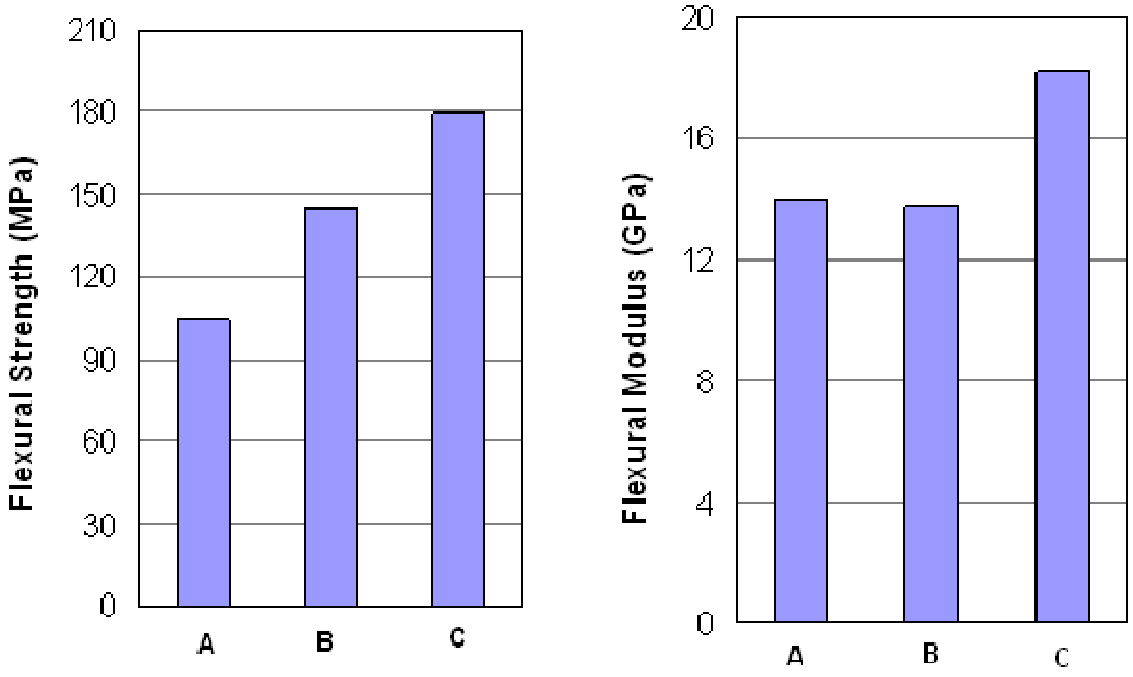

Figure 4.6 Effect of Fiber Surface Treatments on the Flexural Strength and Modulus of the Carbon Fiber/Epoxy Composites.

A: As-received; **B**: HNO_3 Treated; and **C**: O_3 Treated Carbon Fibers.

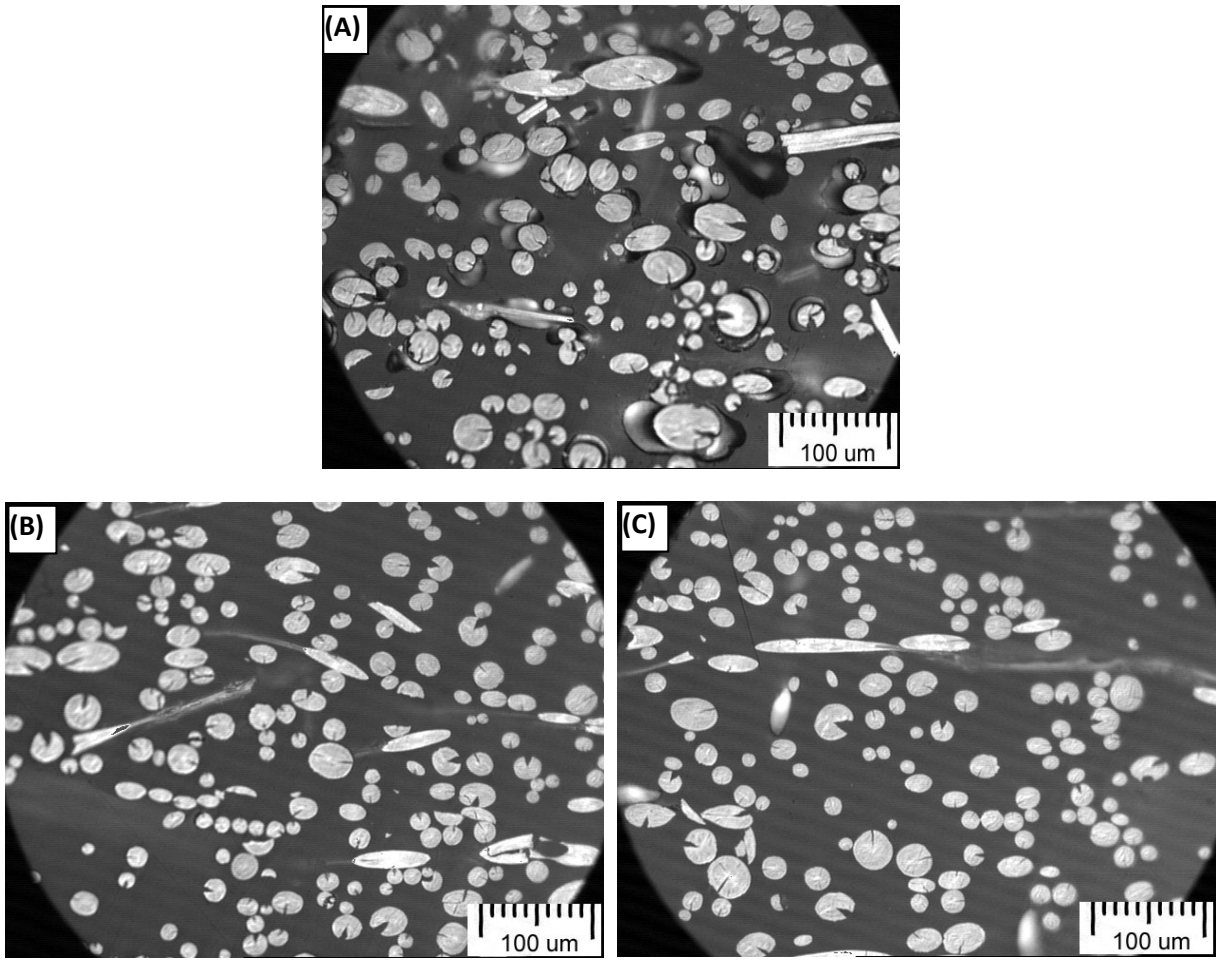

Figure 4.7 Typical Optical Microscopy Images of Epoxy Resin /Carbon Fiber Composites Made from (A): Untreated, (B) HNO_3 Treated, and (C) O_3 Treated Carbon Fibers.

Chapter 5: Conclusion

The main focus of this work is the optimization of the fabrication process for UTSI carbon fiber composites, independent of the quality and production of the CF itself. It is the preliminary work for which future research will be based and improved upon. Several optimization processes such as VBRI, were used to include a slower hardener, variable pressure, and a variety of matrix material. Surface treatment prior to the fabrication of the composite was also found to significantly improve the mechanical characteristics of UTSI CFC's.

VBRI proved the optimal method for controlling porosity. The hot press used in the fabrication process also proved good for controlling fiber volume. The pressures applied compressed the fibers to provide a 6% higher apparent density as compared with VB. The heat applied by press decreased the viscosity to such a degree that it shortened the fabrication time and allowed greater pressures to be applied.

The use of a slower hardener, #209, not only allowed significantly more time for the infusion of the resin into the mold but also allowed relatively higher temperatures of ~ 40°C to be used to decrease the viscosity. The combination of heat and timing allowed the resin to easily diffuse into the mold and gasses to diffuse out.

With the knowledge that the mechanical properties of CFC's are proportional to their fiber volume; we attempted to control the fiber volume by applying pressure. Initial fabrication techniques showed that atmospheric pressures alone would not condense the fibers in a manner which would maximize their volume as compared with the matrix material. An optimal pressure range between 0.5 and 1.0 MPa was also discovered for the certain patch of UTSI carbon fibers studied to provide the best flexural strength and modulus. Pressure increases fiber content/volume by compressing the webbing but pressures beyond the optimal range damage the fibers and decrease flexural strength.

The best flexural strength is obtained with pressures around 0.75 MPa producing flexural strengths greater than 120 MPa.

Apparent density proved to be a good indicator of the ratio between carbon fiber and resin. It also reflects the porosity in the composite material. Apparent density increased with increasing pressure below 1.13 Mpa but lowered afterwards. The two main causes for this characteristic were 1) that pressures beyond the optimum specified crushed the fibers and forces out excess resin and fiber fragments; 2) too much pressure trapped gaseous pockets and slowed the diffusion process to such a degree that air pockets lacked sufficient time to escape.

The overall relationship between volume and electrical conductivity was found to be linear since carbon fibers are conductive. In sum the higher the fiber volume the lower the resistivity. High pressure not only provides high content of fiber but also makes high contact efficiency among the individual fibers. It is sensitive to the amount of pressure used. Pressures at 1.13 Mpa produce CFC with high resistivity. Fibers were crushed and not compressed enough to provide adequate contact from fiber to fiber, reducing contact efficiency. Higher pressure would be necessary to complete the bridge.

The majority of work conducted for this research was done using epoxy resin. Epoxy resin is ideal for the indented uses of the material in mind. The mechanical properties are generally good. Unfortunately it's cost is relatively high and its heat resistance is poor. Preliminary work was done using a low-cost phenolic resin which can also be used to produce C/C composites.

Phenolic resin has an inherent risk of trapping gasses during the curing process. To eliminate this problem a degassing process must be followed. The degas process eliminates the vapors emitted from the solvents and allows more room for matrix material. Without this process the only possible densities are lower than 1 g/cm^3. With degassing apparent densities can be as high as 1.3 g/cm^3. Flexural testing also revealed that degassing is essential in creating high quality CFC's. It decreased voids

and higher apparent density provides greater conductivity and flexural strength and modulus.

C/C composites were created by heating phenolic resin based CFCs at temperatures beyond 1000°C in N_2. Large amounts of defects occurred during the carbonization process due to the decay of non carbon elements. The result was significantly lower apparent densities but higher conductivity. This caused a decrease in flexural strength and modulus. This is expected since the defects serve as points of failure throughout the composite. Successive phenolic resin coatings and carbonization can help fill these voids and solve this problem.

Further structural property analysis revealed poor bonding between the fibers and matrix material. SEM images of epoxy resin CFCs revealed deboning and fiber pull out. This demonstrated a need for a better CFC fabrication method. X-ray diffraction revealed that carbonization at 1050°C provides UTSI mesophase pitch-based carbon fibers with perfect crystalline structure. This means the fiber surface is inherently inert making it difficult to bond with polymer resins. To improve surface bonding surface treatment is essential.

Oxidative surface treatments such as ozone oxidation and liquid phase oxidation in HNO_3 solution were performed for comparison and optimization. It was hoped that by maximizing the bonding strength between the fibers and the matrix material that the mechanical properties of UTSI CFCs will be improved as well.

To quantify the effects of surface treatment single-fiber tensile and diameter strengths were tested. This provided two pieces of information for calculation of the Critical length and IFSS. Single fiber fragmentation tests were performed to characterize the bonding strength by calculating two important pieces of information; 1) critical length, and 2) IFSS. Optical microscope was used to measure the means of fragmentation between the fiber and matrix. It also allowed the degree of adhesion to be easily detected visually by counting the amount of interface patterns using polarized light.

Analysis demonstrated an increase in IFSS in the samples upon oxidation. Initial untreated samples possessed less fragmentation points and more slips due to debonding (**Figures 4.1 - 4.4**). The increase in IFSS from 6.08 Mpa in as-received UTSI CF to 10.73 in HNO_3 and 12.0 in O_3 treatments indicates an improvement in carbon fiber surface properties. The critical lengths also decreased, demonstrating better bonding. The optimal treatment for UTSI CFs appears to be O_3 oxidation because of its smaller average critical length and IFSS compared to HNO_3 treated and as-received CF.

O_3 treated carbon fiber composites also show almost double increase in flexural strength as compared with as received carbon fiber composites.

In conclusion, control of fiber volume and apparent density using VBRI is important for maximizing the mechanical properties of UTSI CFCs. Good control of applied pressure during the curing process is also essential to stay within the optimizational range and avoid damaging fibers. Fiber surface treatment is also very important for producing high performance composites from UTSI mesophase pitch-based CFs. Surface treatment with O_3 proved to be the most effective for UTSI CFs, doubling the flexural strength when compared to as-received CF, and increasing the flexural modulus by 22%.

References

1. Zoltek Corporation, “Carbon Fiber: How It Is Made”.

   http://www.zoltek.com/carbonfiber/made.php

2. M. Khan, A. Barron “Carbon Fibers: Opportunities and Challenges”. Advanced Materials & Processes Vol. 1, p.47 September 2008.

3. M. Schwarz, M. Dekker, “Composite Materials Handbook” McGraw-Hill Inc, 2nd ed December 1992. .

4. H. Hatta, K. Goto, T. Aoki, “Strengths of C/C Composites under Tensile, Shear, and Compressive Loading: Role of Interfacial Shear Strength”. Composites Science and Technology Vol. 65, 2550-2562 August 2005.

5. S. Feih, K. Wonsyld, D, Minzari, P. Westermann, and H. Lilholt, “Testing Procedure for the Single Fiber Fragmentation Test”. Rise National Laboratory, December 2004.

6. P. Morgan, “Carbon Fibers and their Composites”. CRC Press Taylor & Francis Group, 2005.

7. D. L. Chung “Carbon Fiber Composites”. Butterworth-Heinemann, Newton, MA, 1994.

8. W. Callister, “Fundamentals of Material Science and Engineering: An Integrated Approach”. 2nd ed. Wiley, May 2004.

9. ASTM Committee D3039/D3039M “Standard Test Method for Tensile Properties of Polymer Matrix Composite Materials”. ASTM International. January 2006.

10. ASTM Committee D6272 “Standard Test Method for Flexural Properties of unreinforced and Reinforced Plastics and Electrical Insulating Materials by Four Point Bending”. Rev. 9.2 ASTM International. June 2002.

11. P. H. Wang, J. Liu, Z. Yue and R. Y. Li, "Thermal Oxidative Stabilization of Polyacrylonitrile Precursor Fiber--Progression of Morphological Structure and Mechanical Properties". *Carbon*, 1992, 30(1) 113-120.

Appendices

Appendix A: ASTM D 3039/D 3039M, Standard Test Method for Tensile Properties of Polymer Matrix Composite Materials

TABLE 2 Tensile Specimen Geometry Recommendations[A]

Fiber Orientation	Width, mm [in.]	Overall Length, mm [in.]	Thickness, mm [in.]	Tab Length, mm [in.]	Tab Thickness, mm [in.]	Tab Bevel Angle,°
0° unidirectional	15 [0.5]	250 [10.0]	1.0 [0.040]	56 [2.25]	1.5 [0.062]	7 or 90
90° unidirectional	25 [1.0]	175 [7.0]	2.0 [0.080]	25 [1.0]	1.5 [0.062]	90
balanced and symmetric	25 [1.0]	250 [10.0]	2.5 [0.100]	emery cloth	—	—
random-discontinuous	25 [1.0]	250 [10.0]	2.5 [0.100]	emery cloth	—	—

[A] Dimensions in this table and the tolerances of Fig. 2 or Fig. 3 are recommendations only and may be varied so long as the requirements of Table 1 are met.

$$L_{min} = F^{tu}h/2F^{su} \quad (4)$$

where:

L_{min} = minimum required bonded tab length, mm [in.];
F^{tu} = ultimate tensile strength of coupon material, MPa [psi];
h = coupon thickness, mm [in.]; and
F^{su} = ultimate shear strength of adhesive, coupon material, or tab material (whichever is lowest), MPa [psi].

8.2.2.7 *Bonded Tab Adhesive*—Any high-elongation (tough) adhesive system that meets the environmental requirements may be used when bonding tabs to the material under test. A uniform bondline of minimum thickness is desirable to reduce undesirable stresses in the assembly.

8.2.3 *Detailed Examples*—The minimum requirements for specimen design discussed in 8.2.1 are by themselves insufficient to create a properly dimensioned and toleranced coupon drawing. Dimensionally toleranced specimen drawings for both tabbed and untabbed forms are shown as examples in Fig. 2 (SI) and Fig. 3 (inch-pound). The tolerances on these drawings are fixed, but satisfy the requirements of Table 1 for all of the recommended configurations of Table 2. For a specific configuration, the tolerances on Fig. 2 and Fig. 3 might be able to be relaxed.

8.3 *Specimen Preparation*:

8.3.1 *Panel Fabrication*—Control of fiber alignment is critical. Improper fiber alignment will reduce the measured properties. Erratic fiber alignment will also increase the coefficient of variation. The specimen preparation method shall be reported.

8.3.2 *Machining Methods*—Specimen preparation is extremely important for this specimen. Mold the specimens individually to avoid edge and cutting effects or cut from them plates. If they are cut from plates, take precautions to avoid notches, undercuts, rough or uneven surfaces, or delaminations caused by inappropriate machining methods. Obtain final dimensions by water-lubricated precision sawing, milling, or grinding. The use of diamond tooling has been found to be extremely effective for many material systems. Edges should be flat and parallel within the specified tolerances.

10. Conditioning

10.1 *Standard Conditioning Procedure*—Unless a different environment is specified as part of the experiment, condition the test specimens in accordance with Procedure C of Test Method D 5229/D 5229M and store and test at standard laboratory atmosphere (23 ± 3°C [73 ± 5°F] and 50 ± 10 % relative humidity).

11. Procedure

11.1 *Parameters To Be Specified Before Test*:

11.1.1 The tension specimen sampling method, coupon type and geometry, and conditioning travelers (if required).

11.1.2 The tensile properties and data reporting format desired.

NOTE 5—Determine specific material property, accuracy, and data reporting requirements before test for proper selection of instrumentation and data-recording equipment. Estimate operating stress and strain levels to aid in transducer selection, calibration of equipment, and determination of equipment settings.

11.1.3 The environmental conditioning test parameters.

11.1.4 If performed, the sampling method, coupon geometry, and test parameters used to determine density and reinforcement volume.

11.2 *General Instructions*:

11.2.1 Report any deviations from this test method, whether intentional or inadvertent.

11.2.2 If specific gravity, density, reinforcement volume, or void volume are to be reported, then obtain these samples from the same panels being tension tested. Specific gravity and density may be evaluated by means of Test Methods D 792. Volume percent of the constituents may be evaluated by one of the matrix digestion procedures of Test Method D 3171, or, for certain reinforcement materials such as glass and ceramics, by the matrix burn-off technique of Test Method D 2584. The void content equations of Test Methods D 2734 are applicable to both Test Method D 2584 and the matrix digestion procedures.

11.2.3 Following final specimen machining and any conditioning, but before the tension testing, determine the specimen area as $A = w \times h$, at three places in the gage section, and

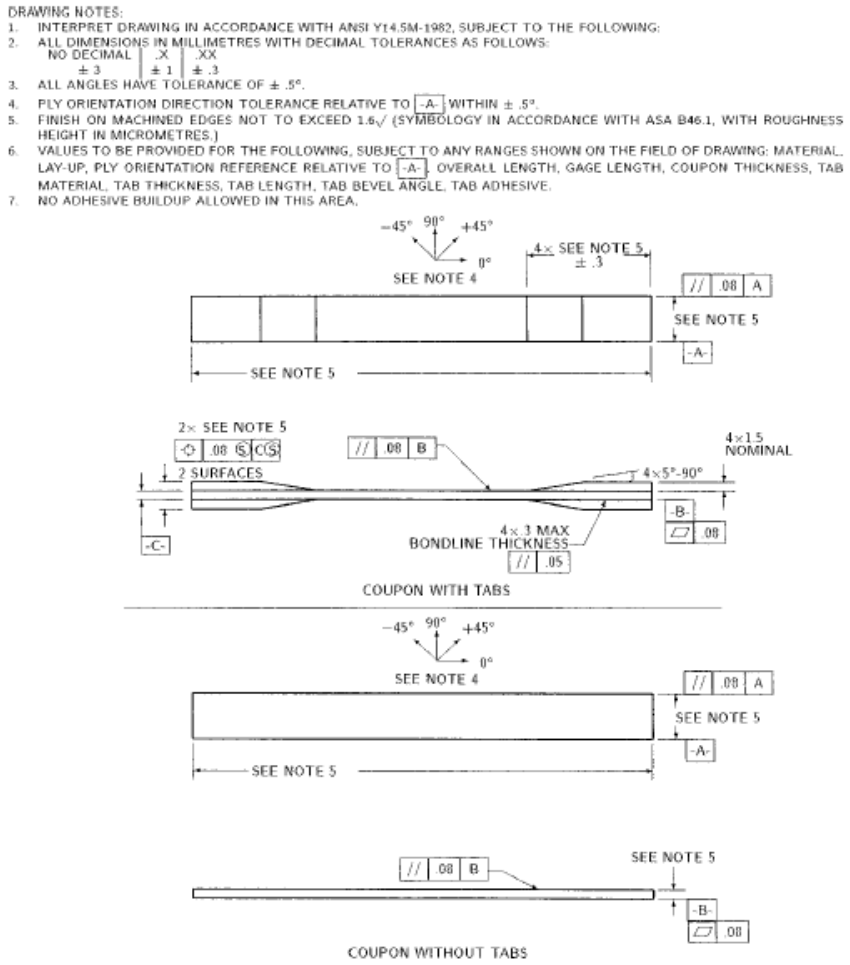

FIG. 2 Tension Test Specimen Drawing (SI)

report the area as the average of these three determinations to the accuracy in 7.1. Record the average area in units of mm^2 ($in.^2$).

11.3 *Speed of Testing*—Set the speed of testing to effect a nearly constant strain rate in the gage section. If strain control is not available on the testing machine, this may be approximated by repeated monitoring and adjusting of the rate of load application to maintain a nearly constant strain rate, as measured by strain transducer response versus time. The strain rate should be selected so as to produce failure within 1 to 10 min. If the ultimate strain of the material cannot be reasonably estimated, initial trials should be conducted using standard speeds until the ultimate strain of the material and the compliance of the system are known, and the strain rate can be adjusted. The suggested standard speeds are:

11.3.1 *Strain-Controlled Tests*—A standard strain rate of 0.01 min^{-1}.

11.3.2 *Constant Head-Speed Tests*—A standard head displacement rate of 2 mm/min [0.05 in./min].

NOTE 6—Use of a fixed head speed in testing machine systems with a high compliance may result in a strain rate that is much lower than required. Use of wedge grips can cause extreme compliance in the system, especially when using compliant tab materials. In some such cases, actual strain rates 10 to 50 times lower than estimated by head speeds have been observed.

11.4 *Test Environment*—Condition the specimen to the desired moisture profile and, if possible, test under the same conditioning fluid exposure level. However, cases such as elevated temperature testing of a moist specimen place unrealistic requirements on the capabilities of common testing machine environmental chambers. In such cases, the mechanical test environment may need to be modified, for example, by testing at elevated temperature with no fluid exposure control, but with a specified limit on time to failure from withdrawal from the conditioning chamber. Modifications to the test environment shall be recorded.

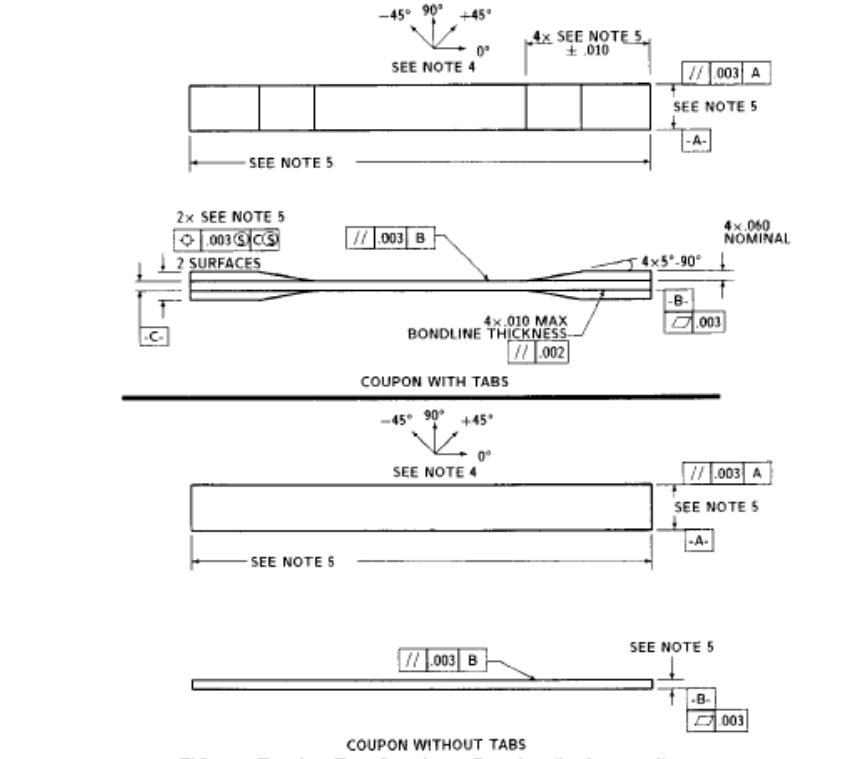

FIG. 3 Tension Test Specimen Drawing (inch-pound)

11.4.1 Store the specimen in the conditioned environment until test time, if the testing area environment is different than the conditioning environment.

11.5 *Specimen Insertion*—Place the specimen in the grips of the testing machine, taking care to align the long axis of the gripped specimen with the test direction. Tighten the grips, recording the pressure used on pressure controllable (hydraulic or pneumatic) grips.

NOTE 7—The ends of the grip jaws on wedge-type grips should be even with each other following insertion to avoid inducing a bending moment that results in premature failure of the specimen at the grip. When using untabbed specimens, a folded strip of medium grade (80 to 150 grit) emery cloth between the specimen faces and the grip jaws (grit-side toward specimen) provides a nonslip grip on the specimen without jaw serration damage to the surface of the specimen. When using tabbed specimens, insert the coupon so that the grip jaws extend approximately 10 to 15 mm [0.5 in.] past the beginning of the tapered portion of the tab. Coupons having tabs that extend beyond the grips are prone to failure at the tab ends because of excessive interlaminar stresses.

11.6 *Transducer Installation*—If strain response is to be determined attach the strain-indication transducer(s) to the specimen, symmetrically about the mid-span, mid-width location. Attach the strain-recording instrumentation to the transducers on the specimen.

11.6.1 When determining modulus of elasticity, it is recommended that at least one specimen per like sample be evaluated with back-to-back axial transducers to evaluate the percent bending, using Eq 5, at the average axial strain checkpoint value (the mid range of the appropriate chord modulus strain range) shown in Table 3. A single transducer can be used if the percent bending is no more than 3 %. When bending is greater

TABLE 3 Specimen Alignment and Chord Modulus Calculation Strain Ranges

Tensile Chord Modulus Calculation Longitudinal Strain Range		Longitudinal Strain Checkpoint for Bending
Start Point	End Point	
με[A]	με	με
1000[B]	3000	2000

[A] 1000 με = 0.001 absolute strain.
[B] This strain range is to be contained in the lower half of the stress/strain curve. For materials that fail below 6000 με, a strain range of 25 to 50 % of ultimate is recommended.

than 3 % averaged strains from back-to-back transducers of like kind are recommended.

$$B_y = \frac{|\epsilon_f - \epsilon_b|}{|\epsilon_f + \epsilon_b|} \quad (5)$$

where:

ϵ_f = indicated strain from front transducer, με;
ϵ_b = indicated strain from back transducer, με; and
B_y = percent bending in specimen.

11.7 *Loading*—Apply the load to the specimen at the specified rate until failure, while recording data.

11.8 *Data Recording*—Record load versus strain (or transducer displacement) continuously or at frequent regular intervals. If a transition region or initial ply failures are noted, record the load, strain, and mode of damage at such points. If the specimen is to be failed, record the maximum load, the failure load, and the strain (or transducer displacement) at, or as near as possible to, the moment of rupture.

NOTE 8—Other valuable data that can be useful in understanding testing anomalies and gripping or specimen slipping problems includes load versus head displacement data and load versus time data.

11.9 *Failure Mode*—Record the mode and location of failure of the specimen. Choose, if possible, a standard description using the three-part failure mode code that is shown in Fig. 4.

11.10 *Grip/Tab Failures*—Reexamine the means of load introduction into the material if a significant fraction of failures in a sample population occur within one specimen width of the tab or grip. Factors considered should include the tab alignment, tab material, tab angle, tab adhesive, grip type, grip pressure, and grip alignment.

12. Calculation

12.1 *Tensile Stress/Tensile Strength*—Calculate the ultimate tensile strength using Eq 6 and report the results to three significant figures. If the tensile modulus is to be calculated, determine the tensile stress at each required data point using Eq 7.

$$F^{tu} = P^{max}/A \quad (6)$$

$$\sigma_i = P_i/A \quad (7)$$

where:

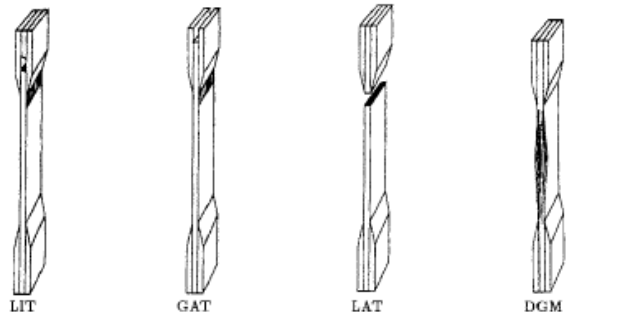

First Character

Failure Type	Code
Angled	A
edge Delamination	D
Grip/tab	G
Lateral	L
Multi-mode	M(xyz)
long. Splitting	S
eXplosive	X
Other	O

Second Character

Failure Area	Code
Inside grip/tab	I
At grip/tab	A
<1W from grip/tab	W
Gage	G
Multiple areas	M
Various	V
Unknown	U

Third Character

Failure Location	Code
Bottom	B
Top	T
Left	L
Right	R
Middle	M
Various	V
Unknown	U

FIG. 4 Tensile Test Failure Codes/Typical Modes

F^{tu} = ultimate tensile strength, MPa [psi];
P^{max} = maximum load before failure, N [lbf];
σ_i = tensile stress at *i*th data point, MPa [psi];
P_i = load at *i*th data point, N [lbf]; and
A = average cross-sectional area from 11.2.3, mm^2 [$in.^2$].

12.2 *Tensile Strain/Ultimate Tensile Strain*—If tensile modulus or ultimate tensile strain is to be calculated, and material response is being determined by an extensometer, determine the tensile strain from the indicated displacement at each required data point using Eq 8 and report the results to three significant figures.

$$\epsilon_i = \delta_i / L_g \tag{8}$$

where:
ϵ_i = tensile strain at *i*th data point, με;
δ_i = extensometer displacement at *i*th data point, mm [in.]; and
L_g = extensometer gage length, mm [in.].

12.3 *Tensile Modulus of Elasticity*:

NOTE 9—To minimize potential effects of bending it is recommended that the strain data used for modulus of elasticity determination be the average of the indicated strains from each side of the specimen, as discussed in 7.3 and 11.6.

Appendix B: ASTM D 6272, Standard Test Method for Flexural Properties of Unreinforced and Reinforced Plastics and Electrical Insulating Materials by Four-Point Bending

specified by contract or the relevant ASTM material specification. Reference testing conditions, to settle disagreements, shall apply tolerances of ±1°C (1.8°F) and ±2 % relative humidity.

10. Procedure

10.1 *Procedure A*:

10.1.1 Use an untested specimen for each measurement. Measure the width and depth of the specimen to the nearest 0.03 mm (0.001 in.) at the center of the support span. For specimens less than 2.54 mm (0.100 in.) in depth, measure the depth to the nearest 0.003 mm (0.0005 in.). These measurements shall be made in accordance with Test Method D 5947.

10.1.2 Determine the support span to be used as described in Section 7 and set the support span to within 1 % of the determined value.

10.1.3 Measure the span accurately to the nearest 0.1 mm (0.004 in.) for spans less than 63 mm (2.5 in.) and to the nearest 0.3 mm (0.012 in.) for spans greater than or equal to 63 mm (2.5 in.). Use the measured span for all calculations. See Annex A2 for information on the determination of and setting of the span.

10.1.4 Calculate the rate of crosshead motion as follows, and set the machine as near as possible to that calculated rate for a load span of one third of the support span:

$$R = 0.185ZL^2/d \quad (1)$$

For a load span of one half of the support span:

$$R = 0.167ZL^2/d \quad (2)$$

where:

R = rate of crosshead motion, mm (in.)/min,
L = support span, mm (in.),
d = depth of beam, mm (in.), and
Z = rate of straining of the outer fibers, mm/mm (in./in.) min. Z shall equal 0.01.

In no case shall the actual crosshead rate differ from Eq 1 or Eq 2, by more than ± 10 %.

10.1.5 Align the loading noses and supports so that the axes of the cylindrical surfaces are parallel and the load span is either one third or one half of the support span. This parallelism may be checked by means of a plate containing parallel grooves into which the loading noses and supports will fit when properly aligned. Center the specimen on the supports, with the long axis of the specimen perpendicular to the loading noses and supports. The loading nose assembly shall be of the type which will not rotate.

10.1.6 Apply the load to the specimen at the specified crosshead rate, and take simultaneous load-deflection data. Measure deflection by a device under the specimen in contact with it at the common center of the spans, the device being mounted stationary relative to the specimen supports. Do not use the movement of the loading noses relative to the supports. Make appropriate corrections for indentation in the specimens and deflections in the weighing system of the machine. Load-deflection curves may be plotted to determine the flexural yield strength, secant or tangent modulus of elasticity, and the total work measured by the area under the load-deflection curve.

10.1.7 If no break has occurred in a specimen by the time the maximum strain in the outer fibers has reached 0.05 mm/mm (in./in.), discontinue the test (Notes 9 and 10). The deflection at which this strain occurs may be calculated by letting r equal 0.05 mm/mm (in./in.) as follows for a load span of one third of the support span:

$$D = 0.21rL^2/d \quad (3)$$

For a load span of one half of the support span:

$$D = 0.23rL^2/d \quad (4)$$

where:

D = midspan deflection, mm (in.),
r = strain, mm/mm (in./in.),
L = support span, mm (in.), and
d = depth of beam, mm (in.).

NOTE 9—For some materials the increase in strain rate provided under Procedure B may induce the specimen to yield or rupture, or both, within the required 5 % strain limit.

NOTE 10—Beyond 5 % strain, these test methods are not applicable, and some other property might be measured (for example, Test Method D 638 may be considered).

10.2 *Procedure B*:

10.2.1 Use an untested specimen for each measurement.

10.2.2 Test conditions shall be identical to those described in 10.1, except that the rate of straining of the outer fibers shall be 0.10 mm/mm (in./in.)/min.

10.2.3 If no break has occurred in the specimen by the time the maximum strain in the outer fibers has reached 0.05 mm/mm (in./in.), discontinue the test (Note 10).

11. Retests

11.1 Values for properties at rupture shall not be calculated for any specimen that breaks at some obvious, fortuitous flaw, unless such flaws constitute a variable being studied. Retests shall be made for any specimen on which values are not calculated.

12. Calculation

NOTE 11—In determination of the calculated value of some of the properties listed in this section it is necessary to determine if the toe compensation (see Annex A1) adjustment must be made. This toe compensation correction shall be made only when it has been shown that the toe region of the curve is due to the takeup of slack, alignment, or seating of the specimen and not an authentic material response.

12.1 *Maximum Fiber Stress*—When a beam is loaded in flexure at two central points and supported at two outer points, the maximum stress in the outer fibers occurs between the two central loading points that define the load span (see Fig. 2). This stress may be calculated for any point on the load-deflection curve for relatively small deflections by the following equation for a load span of one third of the support span (see Notes 12 and 13):

$$S = PL/bd^2 \quad (5)$$

For a load span of one half of the support span:

$$S = 3PL/4bd^2 \quad (6)$$

where:

S = stress in the outer fiber throughout the load span, MPa (psi),
P = load at a given point on the load-deflection curve, N (lbf),
L = support span, mm (in.),
b = width of beam, mm (in.), and
d = depth of beam, mm (in.).

NOTE 12—Eq 5 and 6 apply strictly to materials for which the stress is linearly proportional to strain up to the point of rupture and for which the strains are small. Since this is not always the case, a slight error will be introduced in the use of this equation. The equation will, however, be valid for comparison data and specification values up to the maximum fiber strain of 5 % for specimens tested by the procedure herein described. It should be noted that the maximum stress may not occur in the outer fibers for a highly orthotropic laminate.[5] Laminated beam theory must be applied to determine the maximum tensile stress at failure. Thus, Eq 5 and 6 yield an apparent strength based on homogeneous beam theory. This apparent strength is highly dependent on the ply-stacking sequence for highly orthotropic laminates.

NOTE 13—The above calculation is not valid if the specimen is slipping excessively between the supports.

12.2 *Maximum Fiber Stress, for Beams Tested at Large Support Spans*—If support span-to-depth ratios greater than 16 to 1 are used with resultant deflections in excess of 10 % of the support span occurring, the maximum stress may be reasonably approximated with the following formula for a load span of one third of the support span:

$$S = (PL/bd^2) \cdot [1 + (4.70D^2/L^2) - (7.04Dd/L^2)] \quad (7)$$

For a load span of one half of the support span:

$$S = (3PL/4bd^2) \cdot [1 - (10.91Dd/L^2)] \quad (8)$$

where:
S, P, L, b, and d are the same as for Eq 5, and
D = maximum deflection of the center of the beam, mm (in.).

NOTE 14—When large support span-to-depth ratios are used, significant end forces are developed at the supports which affect the moment in a simply supported beam. An approximate correction factor is given in Eq 7 and 8 to correct for these end forces in large support span-to-depth ratio beams where relatively large deflections exist.

NOTE 15—The limitations defined for Eq 5 and 6 in Notes 13 and 14 apply also to Eq 7 and 8.

12.3 *Flexural Strength*—The flexural strength is equal to the maximum stress in the outer fibers at the moment of break (for highly orthotropic laminates, see Note 12). It is calculated in accordance with Eq 5, Eq 6, Eq 7, and Eq 8 by letting P equal the load at the moment of break. If the material does not break, this part of the test is not applicable. In this case, it is suggested that yield strength, if applicable, be calculated and that the corresponding strain be reported also (see 12.4, 12.6, and 12.7).

12.4 *Flexural Yield Strength*—Some materials that do not break at outer fiber strains up to 5 % may give load-deflection curves that show a point, Y, at which the load does not increase with an increase in deflection. In such cases, the flexural yield strength may be calculated in accordance with Eq 5, or Eq 6 by letting P equal the load at Point Y.

12.5 *Flexural Offset Yield Strength*—Offset yield strength is the stress at which the stress-strain curve deviates by a given strain (offset) from the tangent to the initial straight line portion of the stress-strain curve. The value of the offset must be given whenever this property is calculated.

NOTE 16—This value may differ from flexural yield strength defined in 12.4. Both methods of calculation are described in the annex to Test Method D 638.

12.6 *Stress at a Given Strain*—The maximum fiber stress at any given strain may be calculated in accordance with Eq 5, Eq 6, Eq 7, and Eq 8 by letting P equal the load read from the load-deflection curve at the deflection corresponding to the desired strain (for highly orthotropic laminates, see Note 12).

12.7 *Maximum Strain*—The maximum strain in the outer fibers also occurs at midspan, and it may be calculated as follows for a load span of one third of the support span:

$$r = 4.70Dd/L^2 \quad (9)$$

For load span of one half of the support span:

$$r = 4.36Dd/L^2 \quad (10)$$

where:
r = maximum strain in the outer fibers, mm/mm (in./in.),
D = maximum deflection of the center of the beam, mm
L = support span, mm (in.), and
d = depth, mm (in.).

12.8 *Tangent Modulus of Elasticity*—The tangent modulus of elasticity is the ratio, within the elastic limit, of stress to corresponding strain and shall be expressed in megapascals (pounds per square inch). It is calculated by drawing a tangent to the steepest initial straight-line portion of the load-deflection curve and using Eq 11 for a load span of one third the support span and Eq 12 for a load span of one half of the support span, as follows:

$$E_B = 0.21L^3m/bd^3 \quad (11)$$

$$E_B = 0.17L^3m/bd^3 \quad (12)$$

where:
E_B = modulus of elasticity in bending, MPa (psi),
L = support span, mm (in.),
b = width of beam tested, mm (in.),
d = depth of beam tested, mm (in.), and
m = slope of the tangent to the initial straight-line.

NOTE 17—Shear deflections can seriously reduce the apparent modulus of highly anisotropic composites when they are tested at low span-to-depth ratios.[7] For this reason, a span-to-depth ratio of 60 to 1 is recommended for flexural modulus determinations. Flexural strength should be determined on a separate set of replicate specimens at a lower span-to-depth ratio that induces tensile failures in the outer fibers of the beam along its lower face. Since the flexural modulus of highly anisotropic laminates is a critical function of ply-stacking sequence, it will not necessarily correlate with tensile modulus, which is not stacking-sequence dependent.

12.9 *Secant Modulus of Elasticity*—The secant modulus of elasticity is the ratio of stress to corresponding strain at any given point on the stress-strain curve, or the slope of the straight line that joins the origin and a selected point on the

[7] See Whitney, J. M., et al, "Analysis of the Flexure Test for Laminated Composite Materials," *ASTM STP 546*, 1974, pp. 30–45.

Appendix C. Epoxy Resin Composites Fabricated with VBRI under Pressure of 1 Ton.

Composite description	Entries	Apparent density (g/cm^3)	E-resistivity (Ω*cm)	Flexural Strength (Mpa)	Flexural Modulus (Gpa)
Epoxy/carbon fiber **Applied pressure = 1 Ton**	1	1.30	0.07	118.67	12.39
	2	1.30	0.08	89.56	13.65
	3	1.29	0.08	143.00	16.86
	4	1.22	0.13	82.76	11.02
	5	1.29	0.07	101.76	10.88
	6	1.30	0.08	99.15	12.92
	Average	**1.28**	**0.08**	**105.81**	**12.95**
	St. Dev.	0.031	0.022	21.93	2.19

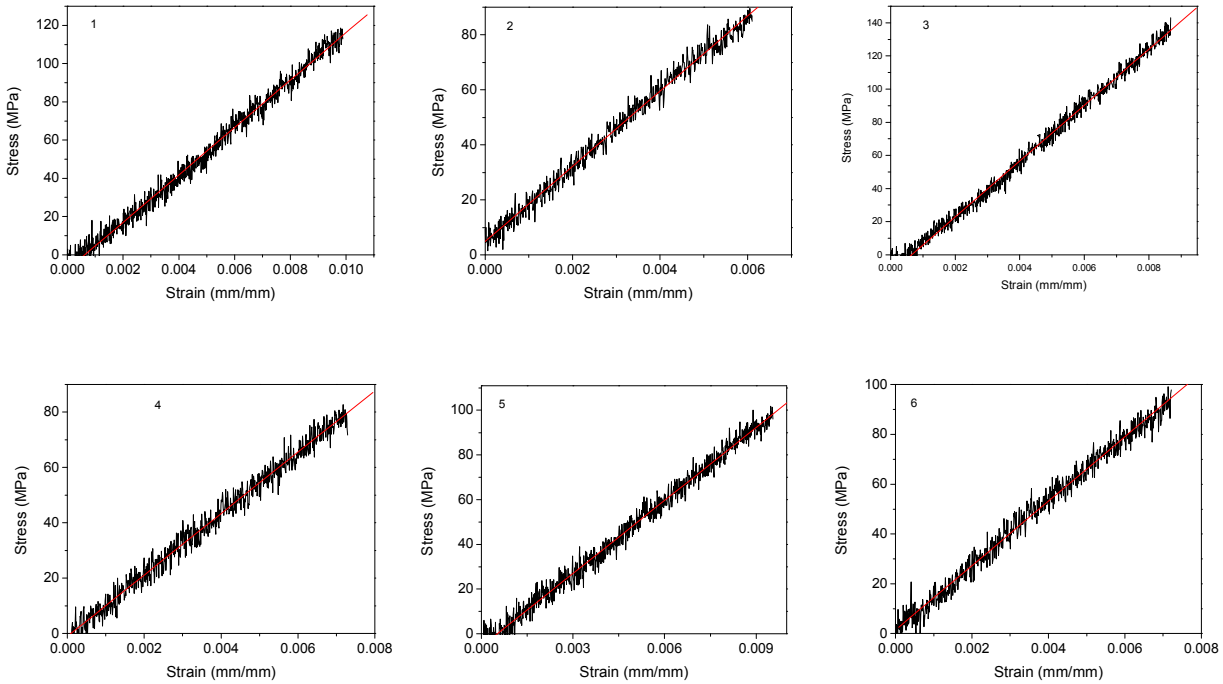

Stress-Strain curves of six composite specimens

Appendix D. Epoxy Resin Composites Fabricated with VBRI under Pressure of 2 Tons.

Composite description	Entries	Apparent density (g/cm^3)	E-resistivity (Ω*cm)	Flexural Strength σ (Mpa)	Flexural Modulus *E* (Gpa)
Epoxy/carbon fiber **Applied pressure = 2 Tons**	1	1.33	0.07	114.80	11.95
	2	1.27	0.04	123.21	11.88
	3	1.30	0.07	108.91	12.00
	4	1.29	0.07	140.88	15.45
	5	1.26	0.05	119.04	13.32
	6	1.31	0.07	132.45	11.62
	Average	**1.29**	**0.06**	**123.21**	**12.7**
	St. Dev.	0.026	0.013	11.75	1.47

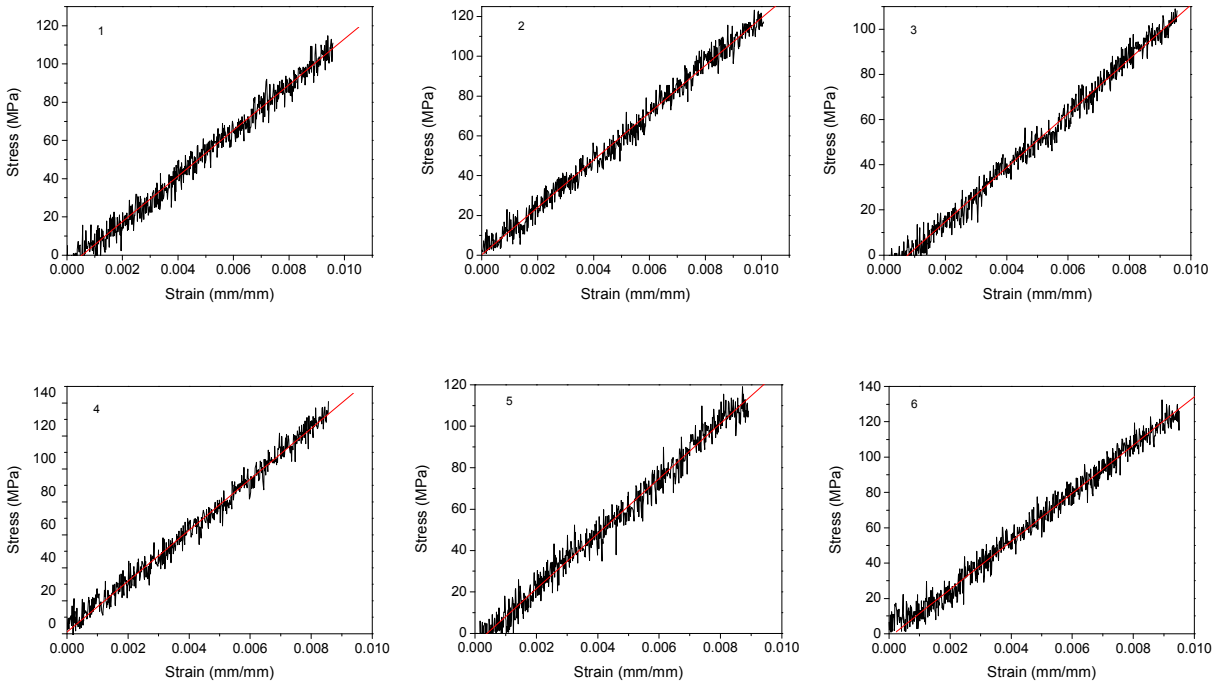

Stress-Strain curves of six composite specimens

Appendix E. Epoxy Resin Composites Fabricated with VBRI under Pressure of 3 Tons.

Composite description	Entries	Apparent density (g/cm^3)	E-resistivity (Ω*cm)	Flexural Strength (Mpa)	Flexural Modulus (Gpa)
Epoxy/carbon fiber **Applied pressure = 3 Tons**	1	1.34	0.07	111.28	14.52
	2	1.38	0.08	96.63	13.25
	3	1.39	0.09	114.13	12.44
	4	1.32	0.10	120.93	17.31
	5	1.30	0.08	99.84	13.77
	6	1.34	0.09	84.29	12.71
	Average	**1.35**	**0.09**	**104.52**	**14.00**
	St. Dev.	0.034	0.010	13.42	1.79

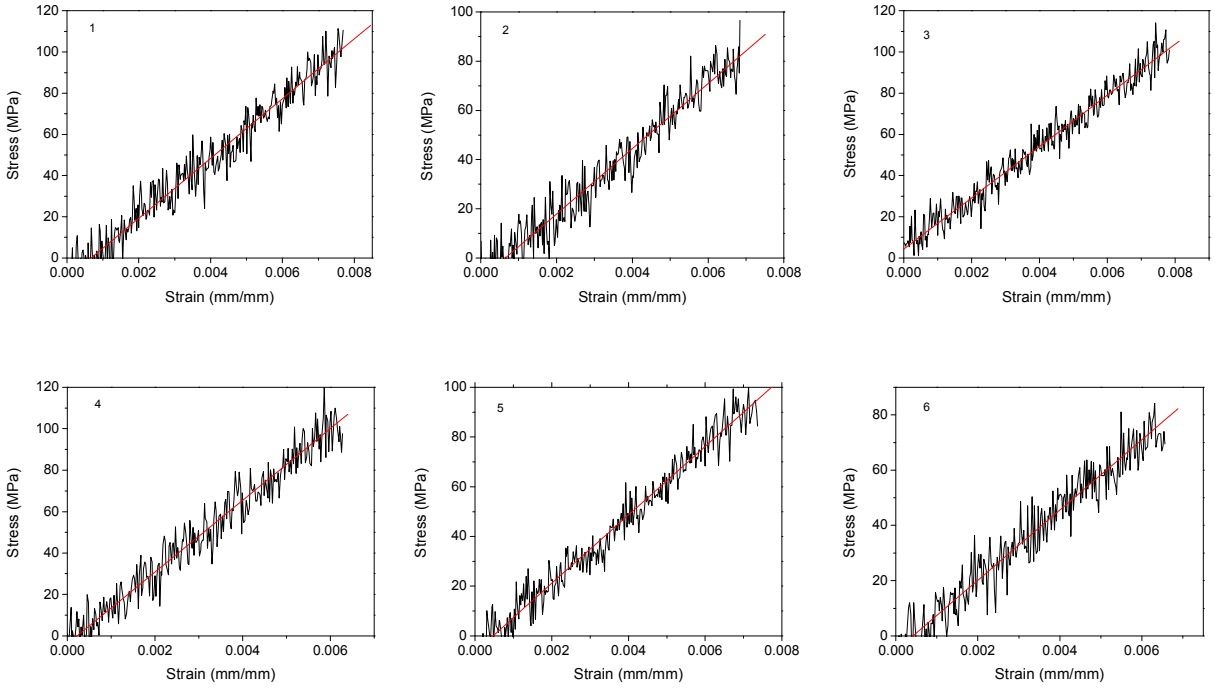

Stress-Strain curves of six composite specimens

Appendix F. Epoxy Resin Composites Fabricated with VBRI under Pressure of 7 Tons.

Composite description	Entries	Apparent density (g/cm^3)	E-resistivity (Ω*cm)	Flexural Strength (Mpa)	Flexural Modulus (Gpa)
Epoxy/carbon fiber **Applied pressure = 7 Tons**	1	1.22	0.03	117.59	15.31
	2	1.30	0.04	113.66	15.74
	3	1.28	0.04	113.65	14.95
	4	1.26	0.04	127.23	15.32
	5	1.23	0.03	160.83	20.47
	6	1.25	0.03	119.05	15.39
	Average	**1.26**	**0.04**	**125.33**	**16.20**
	St. Dev.	0.030	0.005	18.09	2.11

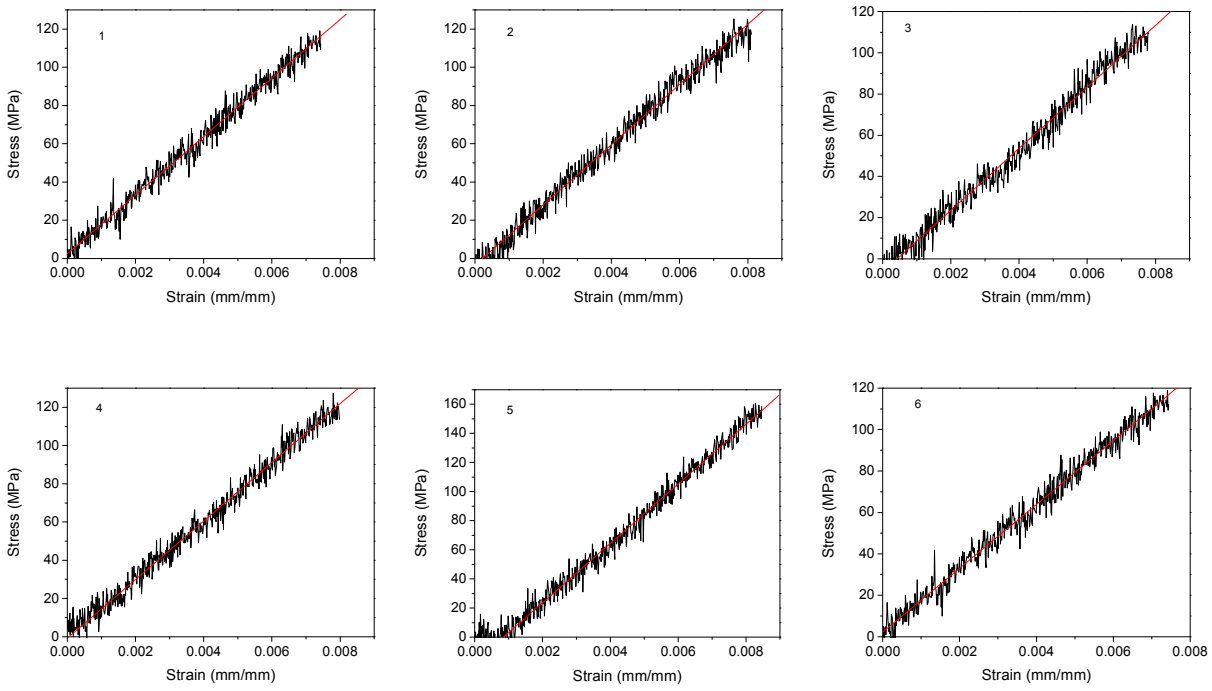

Stress-Strain curves of six composite specimens

Appendix G. Phenolic Resin Composites Fabricated without Degas Process.

Composite description	Entries	Apparent density (g/cm^3)	E-resistivity (Ω*cm)	Flexural Strength (Mpa)	Flexural Modulus (Gpa)
Phenolic resin/carbon fiber	1	1.03	0.07	91.84	12.11
	2	0.99	0.08	67.19	14.18
	3	0.89	0.09	64.24	11.00
Do not degas before heat-crosslinking process	4	0.94	0.08	65.07	12.68
	5	0.97	0.08	82.00	13.77
	6	1.08	0.09	94.99	11.95
	Average	**0.98**	**0.08**	**77.55**	**12.61**
	St. Dev.	0.067	0.007	13.92	1.19

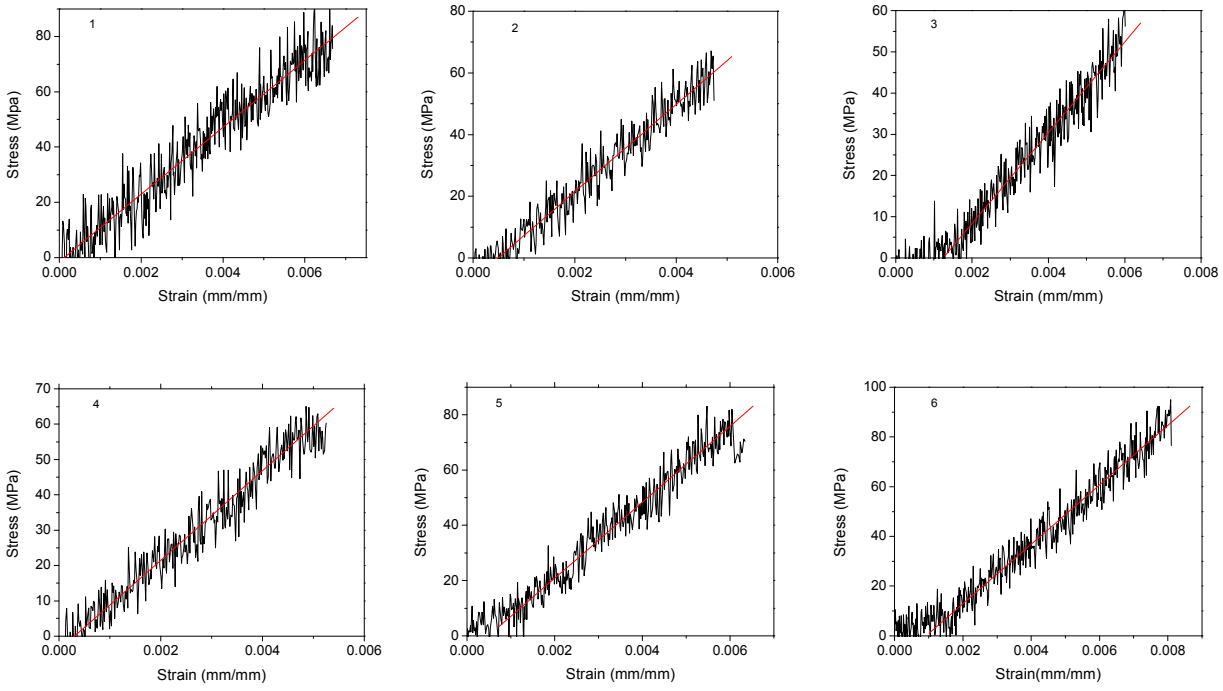

Stress-Strain curves of six composite specimens

Appendix H. Phenolic Resin Composites Fabricated with Degas Process.

Composite description	Entries	Apparent density (g/cm^3)	E-resistivity (Ω*cm)	Flexural Strength (Mpa)	Flexural Modulus (Gpa)
Phenolic resin/carbon fiber **Degas first before heat-crosslinking process**	P1	1.34	0.06	146.57	20.18
	P2	1.34	0.05	126.23	17.15
	P3	1.30	0.04	130.57	19.36
	P4	1.30	0.06	122.27	17.76
	P5	1.30	0.06	116.50	19.53
	P6	1.31	0.05	109.08	17.19
	Average	1.32	0.052	125.20	18.53
	St. Dev.	0.020	0.0082	12.89	1.32

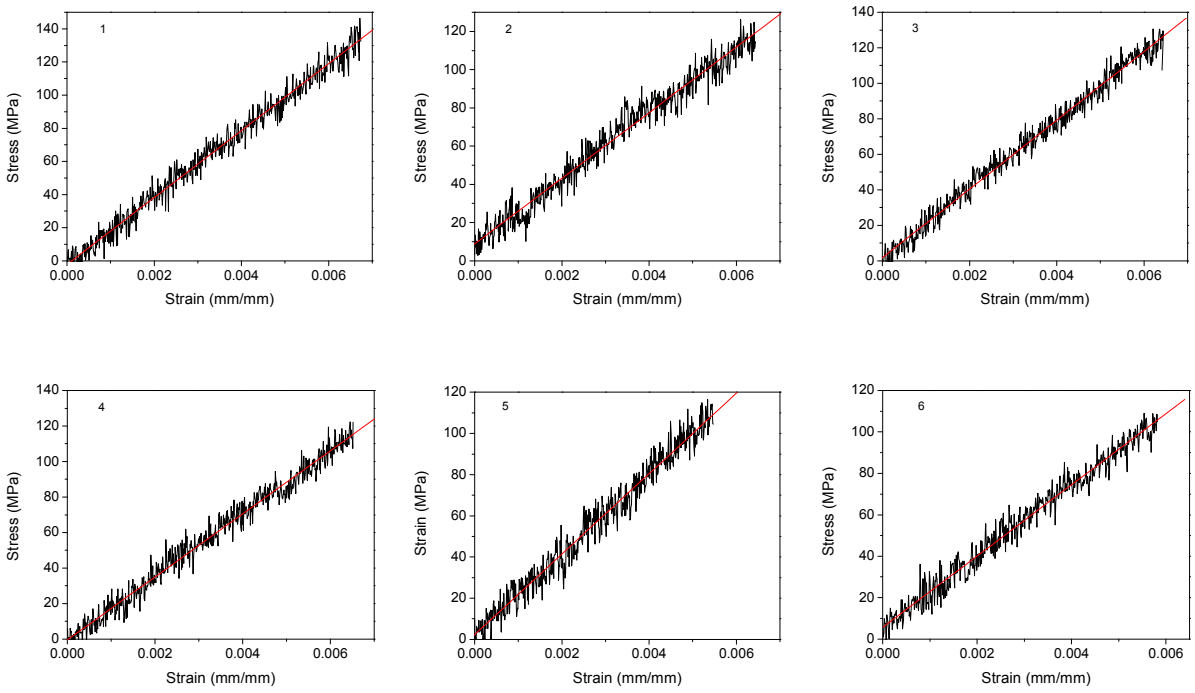

Stress-Strain curves of six composite specimens

Appendix I. Carbon /Carbon Composites Converted from Phenolic Resin Composites with a Carbonization at 1000°C in N_2.

Composite description	Entries	Apparent density (g/cm^3)	E-resistivity (Ω*cm)	Flexural Strength (Mpa)	Flexural Modulus (Gpa)
Carbon/carbon fiber **Converted from phenolic resin composite at 1000°C in N_2**	1	0.95	0.01	35.68	9.82
	2	0.90	0.02	15.59	9.13
	3	0.90	0.02	24.70	5.50
	4	0.92	0.02	27.81	6.97
	5	0.92	0.02	25.85	10.23
	6	0.92	0.02	17.37	6.72
	Average	**0.92**	**0.02**	**24.50**	**8.06**
	St. Dev.	0.018	0.004	7.32	1.92

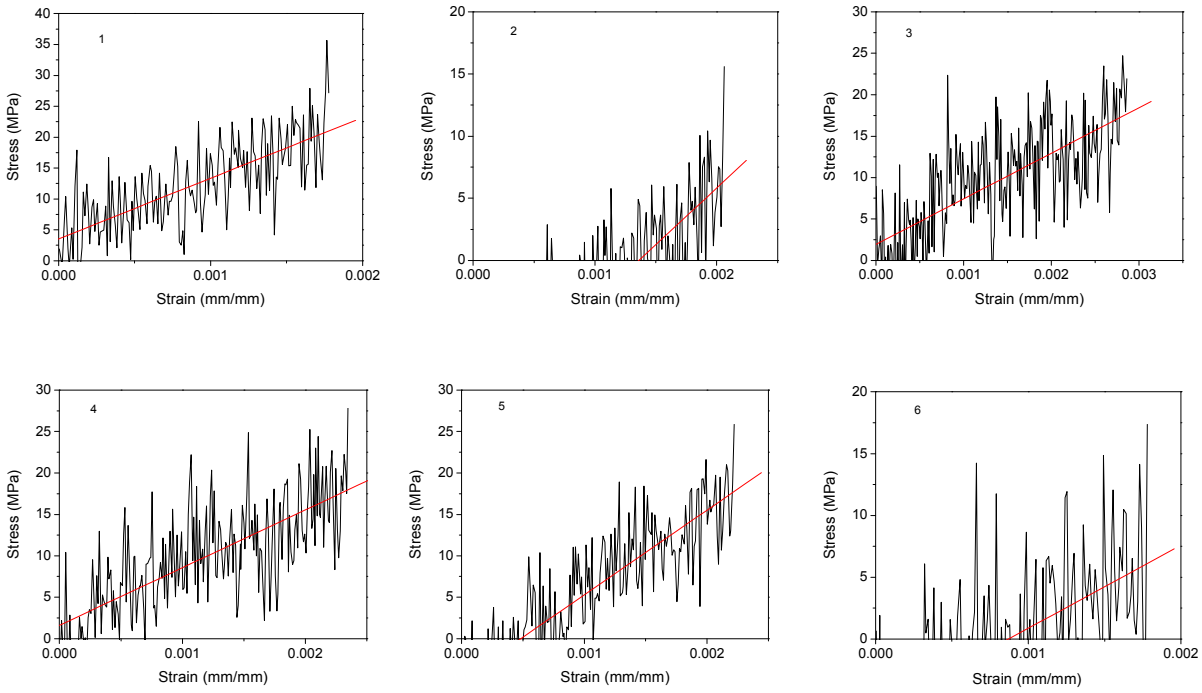

Stress-Strain curves of six composite specimens

Appendix J. Single-fiber Fragmentation Tests

1. As received Carbon Fiber #1

Table A Single- fiber Tensile/Diameter Testing Results.

	Mean Min. Diameter (μm)	Mean Max. Diameter (μm)	Mean Cross-Section (μm^2)	Break Extension (μm)	Break Strength (MPa)
Min.	11.3	11.4	101.5	10426	189.45
Max	13.6	13.7	146.2	11159	986.71
Median	12.3	12.4	120	10527	397.88
Mean	12.4	12.52	122.68	10651	464.95
Std. Dev	0.56	0.584	11.176	203.2	208.70

Table B Single-fiber Fragmentation Testing Results.

Fiber diameter (μm)	Tensile strength (Mpa)	Ave. fragment length (μm)	Critical Length (μm)	IFSS (Mpa)
12.46	464.95	491	654.5	4.4

2. As received Carbon Fiber #2

Table C Single-fiber Tensile/Diameter Testing Results.

	Mean Min. Diameter (μm)	Mean Max. Diameter (μm)	Mean Cross-Section (μm^2)	Break Extension (μm)	Break Strength (MPa)
Min.	17	17.1	229.6	10378	234.13
Max	21.6	21.7	368.3	10513	1227.63
Median	20.2	20.3	322.3	10468	763.3
Mean	19.9	20	314	10454.9	723.1
Std. Dev	1.6	1.6	47.9	43.2	351.8

Table D Single-fiber Fragmentation Testing Results.

Fiber diameter (μm)	Tensile strength (Mpa)	Ave. fragment length (μm)	Critical Length (μm)	IFSS (Mpa)
19.95	723.1	724	965.3	7.4

3. HNO_3 Oxidized Fiber

Table E Single-fiber Tensile/Diameter Testing Results.

	Mean Min. Diameter (μm)	Mean Max. Diameter (μm)	Mean Cross-Section (μm^2)	Break Extension (μm)	Break Strength (MPa)
Min.	17.7	17.8	246.6	10470	259.47
Max	19.7	19.8	307.4	10903	1612.9
Median	19.2	19.3	289.2	10573	874.06
Mean	19	19.1	285.2	10610	883.96
Std. Dev	0.6	0.6	17.5	143	464.18

Table F Single-fiber Fragmentation Testing Results.

Fiber diameter (μm)	Tensile strength (Mpa)	Ave. fragment length (μm)	Critical Length (μm)	IFSS (Mpa)
19.05	884.0	596	794.7	10.6

4. O_3 Oxidized Fiber

Table G Single-fiber Tensile/Diameter Testing Results.

	Mean Min. Diameter (μm)	Mean Max. Diameter (μm)	Mean Cross-Section (μm^2)	Break Extension (μm)	Break Strength (MPa)
Min.	17.5	17.6	242.5	10570	148.69
Max	20.3	20.4	326.3	10844	1208.17
Median	19.3	19.4	294.95	10737.5	734.17
Mean	19.1	19.2	289.68	10722.25	706.30
Std. Dev	1.19	1.19	35.41	122.58	527.52

Table H Single-fiber Fragmentation Testing Results.

Fiber diameter (μm)	Tensile strength (Mpa)	Ave. fragment length (μm)	Critical Length (μm)	IFSS (Mpa)
19.15	706.3	450	600.0	11.3

Appendix K. HNO_3 Oxidized UTSI Carbon Fiber / Epoxy Resin Composites Fabricated with VBRI under Pressure of 3 Tons.

Composite description	Entries	Apparent density (g/cm^3)	E-resistivity (Ω*cm)	Flexural Strength (Mpa)	Flexural Modulus (Gpa)
Epoxy/carbon fiber	1	1.39	0.06	148.02	14.62
	2	1.39	0.07	157.14	16.99
	3	1.37	0.10	118.70	13.28
Fiber was treated with HNO_3 at 100°C for 30 min	4	1.37	0.11	148.14	13.13
	5	1.33	0.28	129.24	12.74
	6	1.43	0.11	169.72	11.93
	Average	**1.38**	**0.12**	**145.16**	**13.78**
Applied pressure = 3 Tons	St. Dev.	0.033	0.080	18.53	1.80

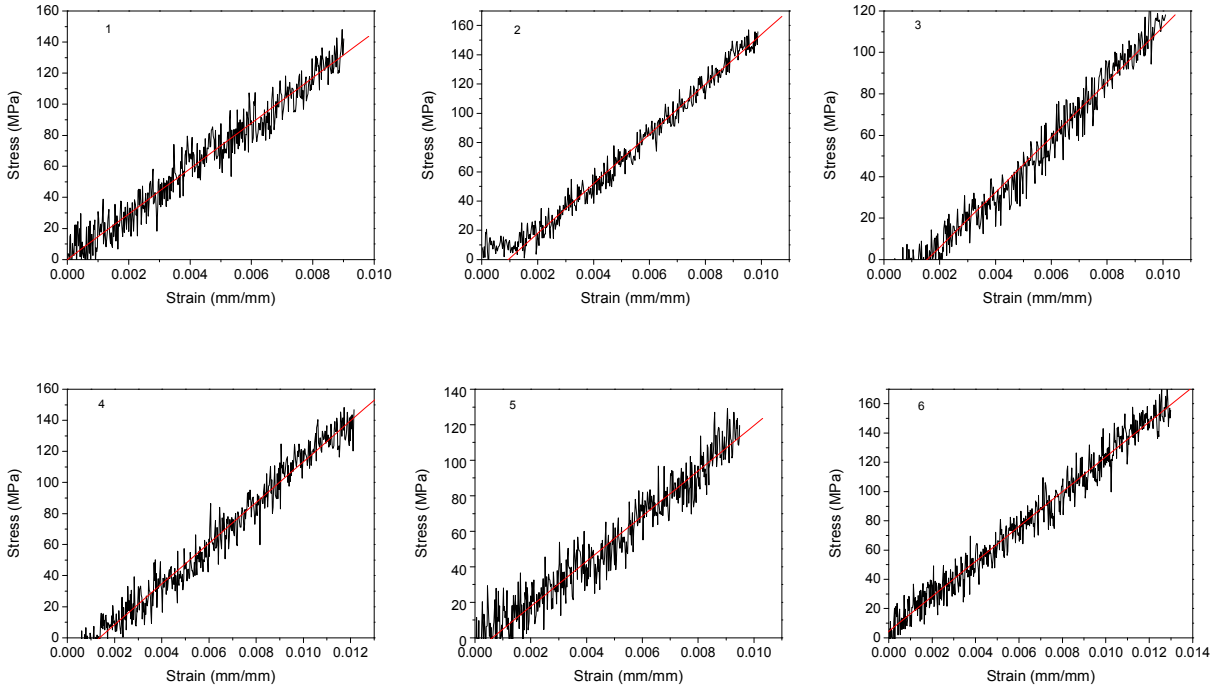

Stress-Strain curves of six composite specimens

Appendix L: O_3 Oxidized UTSI Carbon Fiber / Epoxy Resin Composites Fabricated with VBRI under Pressure of 3 Tons.

Composite description	Entries	Apparent density (g/cm^3)	E-resistivity (Ω*cm)	Flexural Strength (Mpa)	Flexural Modulus (Gpa)
Epoxy/carbon fiber	1	1.27	0.09	137.88	13.84
	2	1.34	1.10	175.36	19.38
	3	1.29	0.13	177.86	14.70
Fiber was treated with O_3 at 200°C for 60 min.	4	1.36	0.09	228.18	24.30
	5	1.33	0.13	204.85	19.92
	6	1.36	0.13	154.48	17.07
	Average	**1.33**	**0.28**	**179.77**	**18.20**
Applied pressure = 3 Tons	St. Dev.	0.037	0.403	32.83	3.85

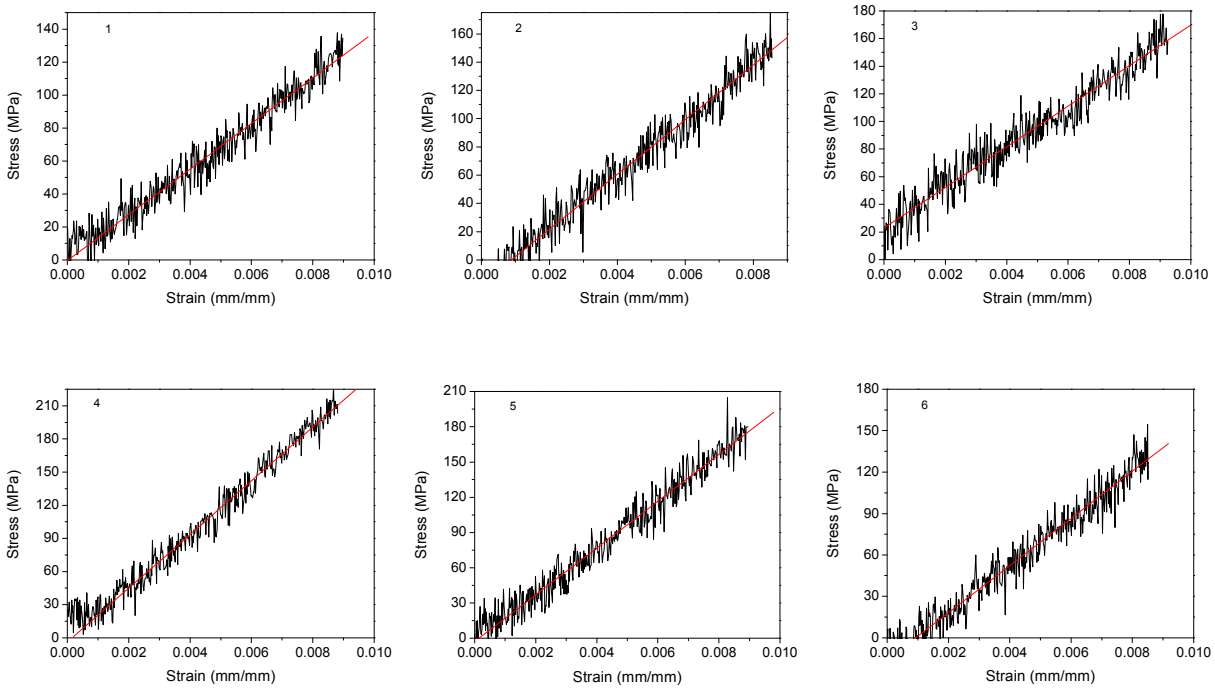

Stress-Strain curves of six composite specimens

Vita

Matthew Patrick Duran was born in Kansas City, Missouri on July 11, 1982. He received his undergraduate degree at Rockhurst University, Kansas City, Missouri in May 2004 attaining a double major in Physics and Mathematics with minor in Philosophy. From Spring 2003 to Spring 2004 he worked as a Lab Technician for Quintiles' physical stability team, Missouri. In June 2004 he joined the University of Tennessee Space Institute as Graduate Research Assistant to pursue a Doctor of Philosophy degree in Theoretical Physics.

He is currently finishing his second Masters in Mechanical engineering and plans on continuing his Ph. D in Physics in the near future.